

# A Stable Measure for Conditional Periodicity of Time Series using Persistent Homology

Bala Krishnamoorthy<sup>\*1</sup> and Elizabeth P. Thompson<sup>†1</sup>

<sup>1</sup>Department of Mathematics and Statistics, Washington State University, USA

## Abstract

We study how the topology of a pair of time series can be used to quantify how similar their periodicities are. Among the known methods to compare a pair of time series, the widely used measure of percent determinism (%DET) requires multiple input parameters. We experimentally show that its many input parameters reduce the stability of %DET.

Persistent homology has been utilized to construct a scoring function with theoretical guarantees of stability that quantifies the periodicity of a single univariate time series  $f_1$ , termed  $\text{score}(f_1)$ . Building on this concept, we propose a conditional periodicity score to quantify the periodicity similarity of a time series  $f_1$  given another more periodic series  $f_2$ , denoted  $\text{score}(f_1|f_2)$ , and derive theoretical results on its stability. This measure uniquely requires only one input parameter. For large embedding dimensions, pairwise distances between points may start to concentrate. With this setting in mind, we prove a new stability result for  $\text{score}(f_1|f_2)$  under principal component analysis (PCA) when we use the projections of the time series embeddings onto their respective first  $K$  principal components. We bound the change in our score by a function of the eigenvalues corresponding to the remaining (unused)  $N - K$  principal components, which is small when the first  $K$  principal components capture most of the variation in the time series embeddings. We derive a lower bound on the minimum embedding dimension to use in our pipeline which guarantees that any two such higher-valued embeddings give scores that are within  $\epsilon$  of each other. Finally, we use this lower bound to further show that small changes in  $\epsilon$  induce small changes in the resulting minimum embedding dimensions.

We present a procedure to compute conditional periodicity scores and implement it on several pairs of synthetic signals. We experimentally compare our similarity measure to %DET, and show its greater stability under small changes in noise, input parameters, and periodicity.

**Keywords:** time series, conditional periodicity, persistent homology, PCA.

---

<sup>\*</sup>kbala@wsu.edu

<sup>†</sup>elizabeth.thompson1@wsu.edu, corresponding author

# 1 Introduction

A continuous univariate time series  $f : T \rightarrow \mathbb{R}$  defined on the real-valued interval  $T$  is a collection of points  $\{(t, f(t))\}$  that depend on the input measure of time,  $t \in T$ . Time series analysis is employed in numerous applications and measuring the similarity between pairs of univariate time series is a well-studied problem. The time shift between a pair of time series can be estimated via the cross-correlation coefficients for a range of self-selected lags. Such coefficients have been used to measure the intensity of earthquakes and identify common significant periods between nucleic signals [13]. The correlation between the power spectra of two time series at a given frequency can be measured using coherence, which has been used to estimate the correlation between non-stationary EEG and EMG signals [27], to detect short significant coherence between non-stationary neural signals [15], and to identify the correlation between green investment and environmental sustainability in China [28]. A non-Euclidean distance between a pair of time series can be measured using dynamic time warping (DTW), a method that does not require a one-to-one correspondence when computing pairwise distances. DTW is commonly used for time-series clustering as it is shown to perform better compared to standard Euclidean distance. DTW has specifically been used to cluster suicidal symptoms signals [9], manic and depressive symptoms signals [18], and marine trafficking signals [25]. The correlation between the point-cloud representations of two time series can be estimated using their pairwise Euclidean distances. Denoted cross-recurrence quantification analysis, this method has been used to quantify the structure of utterance signals between children and their parents [10] and to identify different functional movement levels between patients with and without ACL surgery via EEG and EMG signals [21].

## 1.1 Limitations of Cross-Recurrence

Among the measures previously mentioned, arguably the most popular one is cross-recurrence. For instance, the widely used measure of Percent determinism (%DET) is computed using cross-recurrence, but uses the most self-selected parameters. Cross-recurrence is an asymmetric binary measure that indicates whether or not the  $i$ -th and  $j$ -th states of a pair of time series embeddings are close in Euclidean distance, i.e., cross-recur. See an example of its asymmetry in Figure 1. The collection of all binary cross-recurrence values is summarized in a cross-recurrence matrix,  $\mathcal{C}$ . %DET is the proportion of cross-recurring states that belong to the diagonal strips of ones in  $\mathcal{C}$ , and essentially measures how correlated the embeddings of two series are. %DET requires four self-selected input parameters for its use: the time lag  $\tau$  and embedding dimension  $M$  used to construct the embeddings of both series, the distance threshold  $\text{tol}$  used to determine whether or not a pair of states cross-recur, and the minimum number of points  $\text{minDL}$  in  $\mathcal{C}$  to form a diagonal.

In theory, one would expect %DET to be related to periodicity. For instance, if a pair of time series have close periodicities, then their oscillations sync up more closely. In this case, fixing  $\tau$  and  $M$  should produce time series embeddings that are more correlated (i.e., pairwise distances between the same states should be smaller). For fixed  $\text{minDL}$ , one would further expect %DET to be higher for closer periodicities.

Methods have been introduced for computing optimal parameters for %DET. These include using the auto-mutual information (AMI) of a single time series and Cao's false nearest neighbors (FNN) test to determine the time lag and embedding dimension, and defining  $\tau$  and  $M$  to be either the average or maximum of both lags and dimensions. As well, setting the distance threshold to

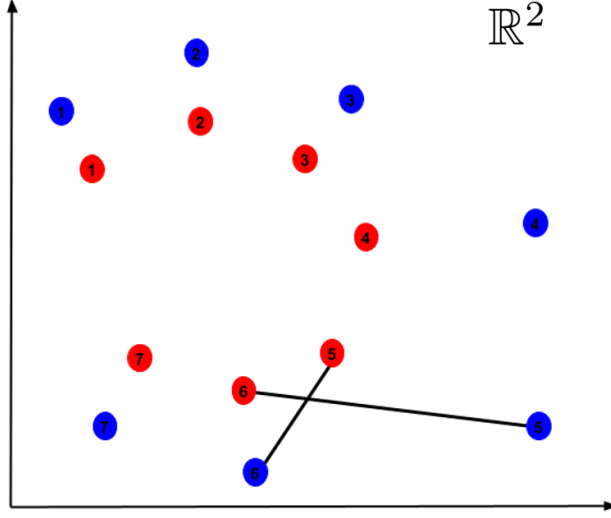


Figure 1: An example of the asymmetry of cross-recurrence where  $\phi_{f_1}(t_i)$  (colored in blue) and  $\phi_{f_2}(t_i)$  (colored in red) denote the  $i$ -th states of the respective embeddings of time series  $f_1$  and  $f_2$  (motivated by Figure 5 in the work of Marwan et al. [16]). Here, since the pairwise Euclidean distances between states  $i = 5$  and  $j = 6$  are not the same, the corresponding entries  $\mathcal{C}_{ij}$  and  $\mathcal{C}_{ji}$  in the cross-recurrence matrix are not necessarily equal. For instance, if we define the distance threshold  $\|\phi_{f_1}(t_5) - \phi_{f_2}(t_6)\|_2 < \text{tol} < \|\phi_{f_1}(t_6) - \phi_{f_2}(t_5)\|_2$ , then  $\mathcal{C}_{56} = 1$  and  $\mathcal{C}_{65} = 0$ .

be greater than five times the standard deviation of Gaussian noise of the input series is a known method to ensure robustness to noise [16]. However, because there are so many parameters involved in computing %DET, periodicity similarity may still not be detected even when using these optimality methods.

For an illustration, we consider in Figure 2 pairs of noisy time series  $f_1$  and  $f_2$  with similar periodicities (first row) and dissimilar periodicities (second and third rows). For both cases, we compute the optimal time lags and dimensions using the AMI and Cao's FNN test for both input series and fix  $\tau$  and  $M$  as the maximum values for each. We fix the Gaussian noise to 5% ( $\sigma = 0.05$ ) and define the distance threshold as  $\text{tol} = 5\sigma + 1.75$ . We first define  $\text{minDL} = 7$  (rows 1 and 2), and then decrease this minimum to  $\text{minDL} = 5$  (row 3). The first column shows a given pair of time series, second column shows the 2D projections of both time series embeddings, and the third column shows the cross-recurrence matrix with %DET value. Notice that %DET is lower in Row 2 (when  $\text{minDL} = 7$ ) as expected, however in Row 3 (when  $\text{minDL} = 5$ ), the periodicity dissimilarity for the same pair of signals is not detected at all by %DET. This illustrates the instability of %DET in detecting periodicity similarity of time series despite the use of optimization techniques.

## 1.2 Our Contributions

Persistent homology frameworks have proven theoretical stability properties [6, 7]. Due to the instability of %DET in detecting periodicity similarity of time series and its many input parameters required, we are motivated to construct a new periodicity similarity measure that uses persistent homology for guaranteed theoretical stability and requires only one self-selected input parameter.

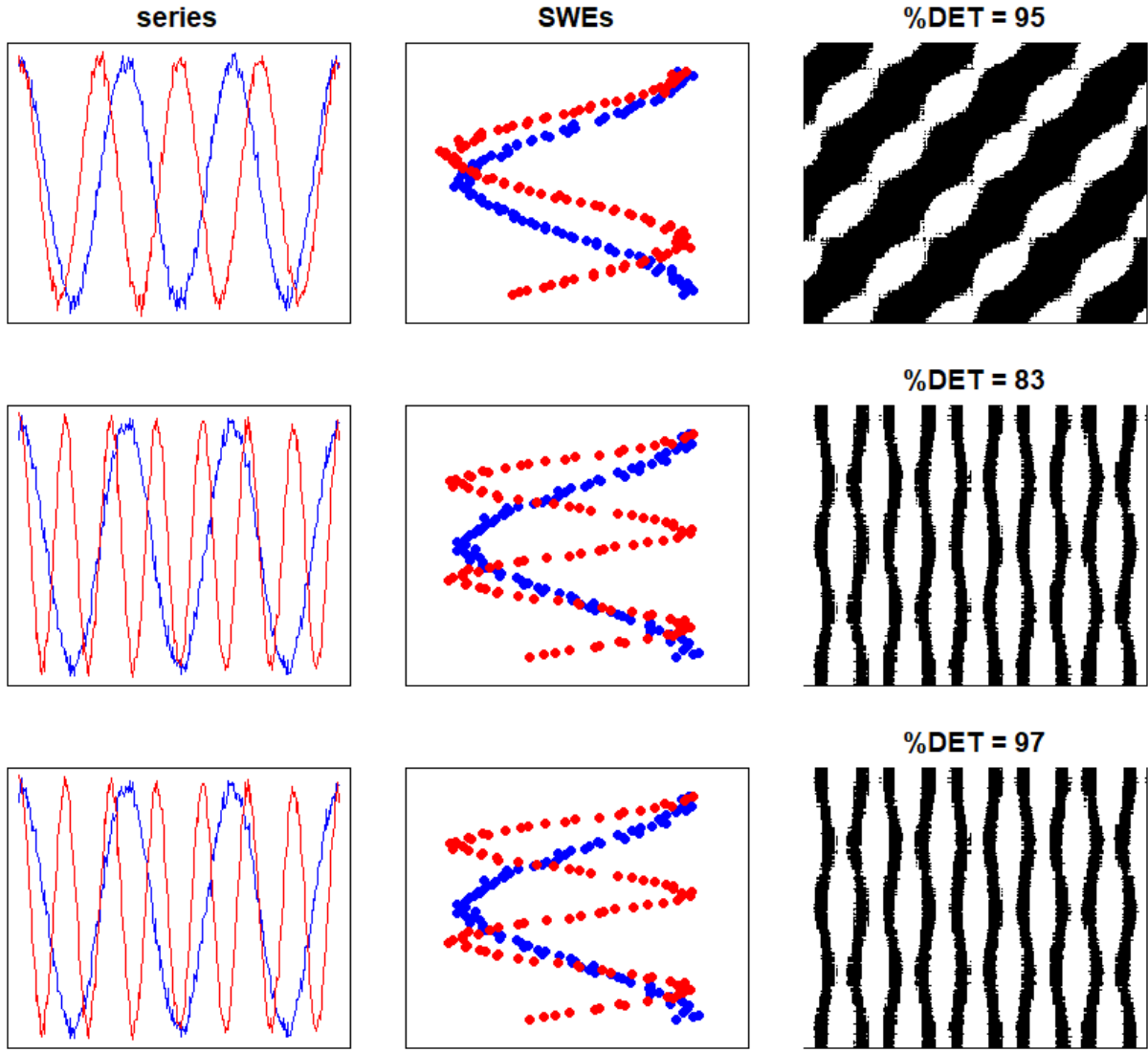


Figure 2: Illustration of the instability of %DET in detecting periodicity similarity. In the first column, we show a pair noisy time series. Column two shows the centered and normalized time series embeddings for these signals. Column three shows the cross-recurrence matrices and percent determinism computed using these embeddings. The top two rows show %DET computed for fixed embedding dimension, time lag, distance threshold, and a minimum diagonal line length of 7. Row three shows %DET computed on the same pair of series in Row two, but for the minimum diagonal line length of 5, illustrating the instability of %DET in detecting periodicity similarity.

For a pair of time series  $f_1, f_2 : T \subset \mathbb{R} \rightarrow \mathbb{R}$  for which  $f_2$  is more periodic (i.e., has shorter cycle-length), we define a new periodicity similarity measure score( $f_1|f_2$ ) (Definition 2.7). This measure uses the persistent homology of a single point cloud representation (Definition 2.5) that captures the relationship between the periodicities of  $f_1$  and  $f_2$  to quantify how similar their periodicities (i.e., cycle-lengths) are. We term this measure the *conditional periodicity score of  $f_1$  given  $f_2$* . See Figure 3 for an illustration of the main difference between how %DET and our score are computed.

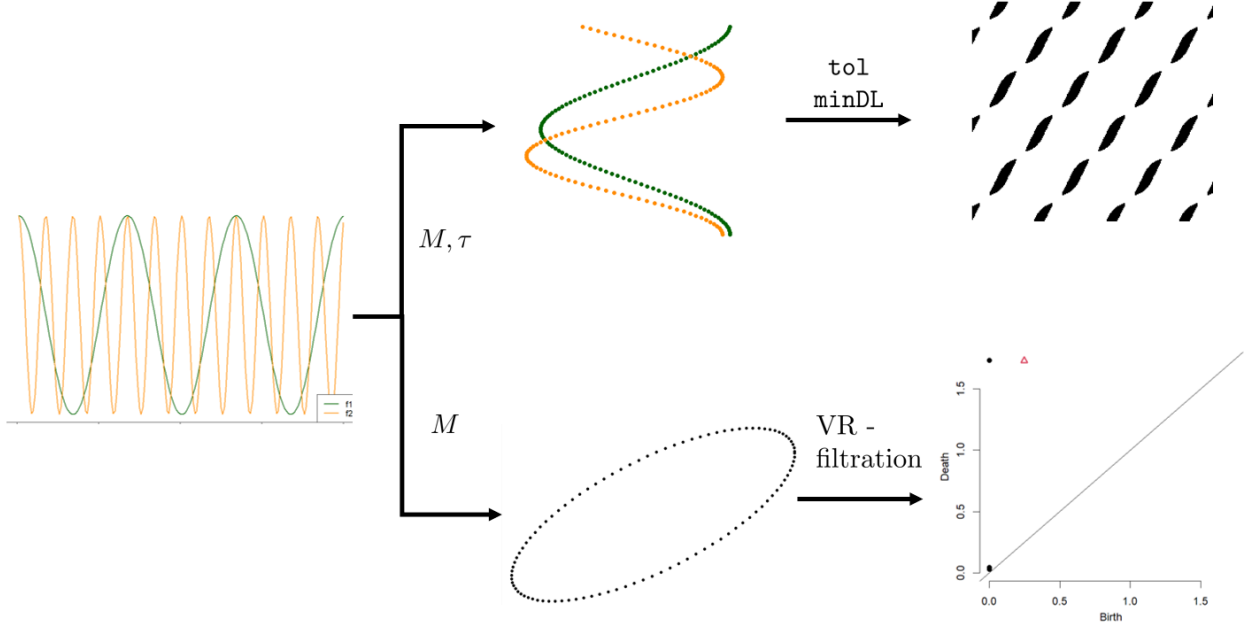


Figure 3: Computation of %DET (top) compared with that of  $\text{score}(f_1|f_2)$  (bottom). The score is computed using the persistence diagram (bottom right) obtained from the VR-filtration of a single point cloud representation (bottom middle) that captures the relationship between the periodicities of both input series (left). This measure requires only one input parameter, the embedding dimension  $M$ . %DET is computed using pairwise Euclidean distances between points in the point cloud representations of both input series (top middle). This measure requires four input parameters, the embedding dimension and time lag ( $M$  and  $\tau$ ) for both time series embeddings, the distance threshold and a minimum number of points to form a diagonal ( $\text{tol}$  and  $\text{minDL}$ ) for the cross-recurrence matrix computation (top right).

The main benefit of our conditional periodicity score as opposed to %DET is its guaranteed theoretical stability under small changes in periodicity (Theorem 3.2) and Gaussian noise (Lemma 3.3) as well as requiring only one input parameter, the embedding dimension  $M \in \mathbb{N}$ . Furthermore, in the context of time series analysis under dimension reduction, we show that our score satisfies a stability result even when one uses truncated versions of the time series embeddings as computed by principal component analysis (PCA) (Theorem 3.4 and Corollary 3.5). We derive a lower bound on the embedding dimension used that allows us to control the precision of the conditional periodicity score (Theorem 3.6), as well as on the number of embedding points to use to capture the difference in periodicities of  $f_1$  and  $f_2$  (Proposition 3.8). Finally, we show in Corollary 3.7 that small changes in desired precision induce small changes in the minimum embedding dimension derived in Theorem 3.6.

Additionally, we highlight the relationship between our stability and convergence results (Section 3.3). The main difference we discuss is that although our periodicity and noise stability results (Theorem 3.2 and Proposition 3.3) show that small increases in periodicity of  $f_2$  or Gaussian noise of  $f_1$  induce small changes in conditional periodicity score, this does not guarantee that the scores being produced are “close” to the underlying conditional periodicity score. This closeness is guaranteed by our convergence result for a minimum choice of embedding dimension (Theorem 3.6). We demonstrate an example of this in Figure 4.

We present an algorithm to quantify the conditional periodicity of two input time series using PCA (Algorithm 1). This algorithm runs in  $O(P \log P + NK^2 + N^2)$  time where  $P$  is the number of points in the two discrete univariate input signals,  $N$  is the number of points in the conditional sliding window embedding (SWE) of the fitted continuous signals, and  $K$  is the number of principal components used ( $K \leq M + 1$  for embedding dimension  $M$ ) (see Remark 4.1). We present computational evidence that shows our scoring function is robust to input signals of different types including sinusoidals, damped sinusoidals, sawtooth-like series, and square-waves with moderate amounts of Gaussian noise and dampening (Figure 6). In addition, our conditional periodicity score, when compared to percent determinism, is shown experimentally to maintain greater stability when subject to small changes in periodicity (i.e., cycle length of  $f_2$ ), Gaussian noise, and input parameters (Figures 7 and 8).

### 1.3 Related Work

As previously mentioned, several similarity measures have been used that indirectly quantify the closeness of periodicities, but we have yet to find any known theoretical stability results for these. These include cross-correlation, coherence, cross-recurrence, and DTW. Persistent homology, on the other hand, has been utilized to quantify the periodicity of a single univariate time series with theoretical stability guarantees [19, 20, 23, 24]. Inspired by the Takens embedding [22], one selects an embedding dimension  $M \in \mathbb{N}$  and a time lag  $\tau > 0$  to map each time-series point  $(t, f(t))$  from a univariate series to an  $(M + 1)$ -dimensional vector via the map

$$\text{SW}_{M,\tau} f(t) = \left( f(t), f(t + \tau), \dots, f(t + M\tau) \right)^T.$$

In other words, one maps windows of size  $M\tau$  of the input signal to one vector in a point cloud in  $\mathbb{R}^{M+1}$ . Further, if the series is periodic on  $[0, 2\pi]$ , the resulting point cloud will be an elliptic curve that is roundest when the sliding window size is proportional to the underlying periodicity of the time series. One then performs Vietoris-Rips (VR) filtration on the sliding windows embedding,  $\text{SW}_{M,\tau} f(t)$ . The more periodic the input signal is, the more rounded the sliding windows embedding is. This yields a higher lifetime of the longest-surviving hole, called the maximum 1D-persistence. Dividing this maximum lifetime by the square root of three (assuming the sliding windows embedding (SWE) is centered and normalized) yields a periodicity score between 0 and 1, denoted  $\text{score}(f)$ , where  $\text{score}(f)$  is closer to 1 when  $f$  is more periodic. This periodicity score and its aforementioned properties were introduced by Perea and Harer [19], and further used to quantify the periodicity of gene-expressions data by Perea, Deckard, Haase, and Harer [20].

The authors derive the normalization factor  $1/\sqrt{3}$  for their scoring function in their proof of a lower bound on 1D max persistence [Theorem 6.8, [19]]. That is, they first define a finite

collection of discrete time points  $T = \{t_1, \dots, t_{J-1}, t_J\}$  for a time series  $f : T \rightarrow \mathbb{R}$ , and the pointwise centered and normalized SWE of its  $N$ -truncated Fourier series  $S_N f$  at time  $t \in T$ , a vector in  $\mathbb{R}^{M+1}$  denoted by  $\psi_\tau(t)$ . They further define  $\kappa_N = \frac{2\sqrt{2}\|S_N f'(t)\|_2}{\|S_N(f - \hat{f}(0))\|_2}$ . They then show that if the Hausdorff distance between  $T$  and the set of all input times corresponding to the Torus,  $\mathbb{T} = \mathbb{R}/(2\pi\mathbb{Z})$ , is strictly less than  $\delta$  for  $0 < \delta < \frac{\sqrt{3}\tilde{r}_n}{\kappa_N}$  (i.e.,  $|t_j - t_{j-1}| < 2\delta$ ), then the Euclidean distance between any consecutive pair of vectors  $\psi_\tau(t_{j-1})$  and  $\psi_\tau(t_j)$  in  $\phi_\tau(T)$  is at most  $\delta\kappa_N < \max_{1 \leq n \leq N} \sqrt{3}\tilde{r}_n \leq \sqrt{3}$ , where  $\tilde{r}_n$  the  $n$ -th (normalized) Fourier coefficient. Since the VR-complex of  $\phi_\tau(T)$  is determined by such pairwise Euclidean distances, they fix the maximum filtration scale to  $\epsilon = \sqrt{3}$ . The stability of this scoring function is proven by the authors [19] using the well-known stability result for persistent homology [6, 7]:

$$d_B \left( \text{dgm}(\text{VR}(X)), \text{dgm}(\text{VR}(Y)) \right) \leq 2 d_{\text{GH}}(X, Y) \leq 2 d_H(X, Y) \quad (1)$$

where the finite data sets of points  $X$  and  $Y$  lay in a common metric space. Here,  $\text{dgm}(\text{VR}(X))$  and  $\text{dgm}(\text{VR}(Y))$  denote the persistence diagrams obtained from the VR filtrations on the point clouds  $X$  and  $Y$ , respectively,  $d_B \left( \text{dgm}(\text{VR}(X)), \text{dgm}(\text{VR}(Y)) \right)$  defines the bottleneck distance between persistence diagrams  $\text{dgm}(\text{VR}(X))$  and  $\text{dgm}(\text{VR}(Y))$ ,  $d_{\text{GH}}(X, Y)$  denotes the Gromov-Hausdorff distance between  $X$  and  $Y$ , and  $d_H(X, Y)$  denotes the Hausdorff distance between  $X$  and  $Y$ . Since we use the VR filtration by default in this work, we will write  $\text{dgm}(X)$  in short to denote  $\text{dgm}(\text{VR}(X))$  when there is no cause for confusion.

## 2 Definitions

Here we introduce standard definitions of distances used in this paper. See, for instance, the book by Burago, Bugaro, and Ivanov [5] for details.

**Definition 2.1** (Hausdorff Distance). *Given two sets of points  $X$  and  $Y$  in a common metric space, the Hausdorff distance between them is given by*

$$d_H(X, Y) = \inf \{ \epsilon > 0 : X \subseteq Y^\epsilon, Y \subseteq X^\epsilon \}, \text{ where } X^\epsilon = \bigcup_{x \in X} B_\epsilon(x) \text{ and } Y^\epsilon = \bigcup_{y \in Y} B_\epsilon(y)$$

denote the union of all  $\epsilon$ -balls centered at each point in either set.

**Definition 2.2** (Hausdorff Definition of Gromov-Hausdorff Distance). *Given two sets of points  $X$  and  $Y$ , the Gromov-Hausdorff distance between them is given by*

$$d_{\text{GH}}(X, Y) = \inf \{ d_H(f(X), g(Y)) : f : X \rightarrow S, g : Y \rightarrow S \},$$

where  $f$  and  $g$  are isometric embeddings of  $X$  and  $Y$  into a common metric space  $S$ . If  $X$  and  $Y$  lay in a shared metric space  $S$ , then  $d_{\text{GH}}(X, Y) \leq d_H(X, Y)$  [1].

**Definition 2.3** (Distortion Definition of Gromov-Hausdorff Distance). *An alternative definition of the Gromov-Hausdorff distance between two sets of points  $X$  and  $Y$  is given by*

$$d_{\text{GH}}(X, Y) = \frac{1}{2} \inf \{ \text{dis}(R) : R : X \rightarrow Y \in \mathcal{R}(X, Y) \},$$

where  $R$  is a relation between  $X$  and  $Y$  whose distortion is defined by

$$\text{dis}(R) = \sup \{ |d_X(x, x') - d_Y(y, y')| : (x, y), (x', y') \in R \},$$

where  $d_X$  and  $d_Y$  are the corresponding metrics for  $X$  and  $Y$ , respectively.

**Definition 2.4** (Bottleneck Distance). *Given two finite sets of points  $X$  and  $Y$ , let  $\text{dgm}(X)$  and  $\text{dgm}(Y)$  denote the persistence diagrams of a chosen dimension obtained from the Vietoris-Rips (VR) filtration on  $X$  and  $Y$ , respectively. Then the Bottleneck distance between  $\text{dgm}(X)$  and  $\text{dgm}(Y)$  is given by*

$$d_B(\text{dgm}(X), \text{dgm}(Y)) = \inf_{\phi} \sup_x \|x - \phi(x)\|_{\infty},$$

where  $\phi : \text{dgm}(X) \rightarrow \text{dgm}(Y)$  denotes a bijection between  $\text{dgm}(X)$  and  $\text{dgm}(Y)$ , including points along the diagonal in either diagram when they both do not share the same cardinality.

## 2.1 The Conditional Periodicity Score

We now present the definitions of our measure for the conditional periodicity of two univariate time series.

**Definition 2.5** (Conditional Sliding Windows Embedding). *Let  $f_1, f_2 : [0, 2\pi] \rightarrow \mathbb{R}$  be two continuous, periodic, univariate time series with cycle-lengths  $\frac{2\pi}{w_1}$  and  $\frac{2\pi}{w_2}$ , respectively. Assume  $w_1, w_2 \in \mathbb{N}$ , and that  $\frac{2\pi}{w_2} \leq \frac{2\pi}{w_1}$ . Then the conditional sliding windows embedding (SWE) of  $f_1$  given  $f_2$  is defined by*

$$\text{SW}_{M,\tau} f_{1|2}(t) = \left( f_1(t), f_1(t + \tau), \dots, f_1(t + M\tau) \right)^T$$

where  $M \in \mathbb{N}$  is a selected embedding dimension and the time lag  $\tau = \frac{2\pi}{w_2(M+1)}$  is proportional to the length of one cycle of  $f_2$ .

**Definition 2.6** (Periodic Functions). *A continuous time series  $f : [0, 2\pi] \rightarrow \mathbb{R}$  is  $L$ -periodic if  $f(t + \frac{2\pi}{L}) = f(t)$ ,  $L \in \mathbb{N}$  [19]. Throughout this paper, we denote the cycle length of a time series as its periodicity. We further denote one time series to be more periodic than another if its cycle length is smaller.*

**Definition 2.7** (Conditional Periodicity Score). *Let  $\text{mp}(\text{dgm}_1(\text{SW}_{M,\tau} f_{1|2}(T)))$  denote the lifetime of the longest surviving one-dimensional homology feature (i.e., hole) in the VR filtration on the conditional SWE of  $f_1$  given  $f_2$ . Then the conditional periodicity score of  $f_1$  given  $f_2$  is defined as*

$$\text{score}(f_1|f_2) = \frac{\text{mp}(\text{dgm}_1(\text{SW}_{M,\tau} f_{1|2}(T)))}{\sqrt{3}}$$

for  $T = \left[ 0, \frac{2\pi}{w_1} \right]$ .

### 3 Stability of the Conditional Periodicity Score

To obtain  $\text{score}(f_1|f_2)$ , we first compute the conditional SWE of  $f_1$  given a more periodic series  $f_2$  (Definition 2.5), and then compute the VR filtration of this embedding to obtain the conditional periodicity score (Definition 2.7). Assuming that  $f_2$  is more periodic than  $f_1$ , we ultimately deduce that small changes in the periodicity of  $f_2$  yield small changes in the conditional periodicity score. We assume that  $f_1$  and  $f_2$  are continuous series defined on  $[0, 2\pi]$  where  $f_2$  is more periodic than  $f_1$ , i.e.,  $\frac{2\pi}{w_2} \leq \frac{2\pi}{w_1}$  for  $w_1, w_2 \in \mathbb{N}$ . We also assume that any conditional SWE contains  $N \in \mathbb{N}$  points. We first observe that as the periodicity of  $f_2$  approaches that of  $f_1$ , the conditional periodicity score reduces to the periodicity score of  $f_1$ .

**Proposition 3.1** (Reduction to Periodicity Score).

$$\lim_{\frac{2\pi}{w_2} \rightarrow \frac{2\pi}{w_1}^-} \text{SW}_{M,\tau} f_{1|2}(t) = \text{SW}_{M,\tau} f_1(t) \text{ for } t \in \left[0, \frac{2\pi}{w_1}\right].$$

*Proof.* Let  $i \in \{1, 2, \dots, M+1\}$  for fixed  $M \in \mathbb{N}$ . Since  $f_1$  is continuous and differentiable on  $[0, 2\pi]$  and hence on  $(0, 2\pi)$ , it is continuous and differentiable on any subset  $[a, b] \subset [0, 2\pi]$  and  $(a, b) \subset (0, 2\pi)$ . Let  $t \in [0, 2\pi]$ . Consider the subinterval  $I_i = \left[t + \frac{2(i-1)\pi}{w_2(M+1)}, t + \frac{2(i-1)\pi}{w_1(M+1)}\right]$  of  $[0, 2\pi]$ . Then  $f_1$  is also continuous and differentiable on  $I_i$ . By the Mean Value Theorem (MVT), there exists some  $c_i \in I_i$  such that

$$f'_1(c_i) \left[ \left( t + \frac{2(i-1)\pi}{w_1(M+1)} \right) - \left( t + \frac{2(i-1)\pi}{w_2(M+1)} \right) \right] = f_1 \left( t + \frac{2(i-1)\pi}{w_1(M+1)} \right) - f_1 \left( t + \frac{2(i-1)\pi}{w_2(M+1)} \right).$$

Then we get the following equality:

$$\begin{aligned} & \|\text{SW}_{M,\tau} f_{1|2}(t) - \text{SW}_{M,\tau} f_1(t)\|_2 \\ &= \left( \sum_{i=1}^{M+1} \left| f_1 \left( t + \frac{2(i-1)\pi}{w_2(M+1)} \right) - f_1 \left( t + \frac{2(i-1)\pi}{w_1(M+1)} \right) \right|^2 \right)^{\frac{1}{2}} \\ &= \left( \sum_{i=1}^{M+1} |f'_1(c_i)|^2 \left| \left( t + \frac{2(i-1)\pi}{w_2(M+1)} \right) - \left( t + \frac{2(i-1)\pi}{w_1(M+1)} \right) \right|^2 \right)^{\frac{1}{2}} \\ &= \left( \sum_{i=2}^{M+1} |f'_1(c_i)|^2 \left| \frac{i-1}{M+1} \right|^2 \left| \frac{2\pi}{w_1} - \frac{2\pi}{w_2} \right|^2 \right)^{\frac{1}{2}}. \end{aligned} \quad \square$$

A direct consequence of Proposition 3.1 is that  $\text{score}(f_1|f_2) \rightarrow \text{score}(f_1)$  as  $\frac{2\pi}{w_2} \rightarrow \frac{2\pi}{w_1}^-$ .

**Theorem 3.2** (Stability of Conditional Periodicity Score). *Let  $f_1, f_{21}, f_{22} : [0, 2\pi] \rightarrow \mathbb{R}$  be three continuous univariate time series such that  $\frac{2\pi}{w_{22}} < \frac{2\pi}{w_{21}} \leq \frac{2\pi}{w_1}$  and  $w_1, w_{21}, w_{22} \in \mathbb{N}$ . Define the conditional SWE of  $f_1$  given  $f_{21}$  as  $X_1$  and the conditional SWE of  $f_1$  given  $f_{22}$  as  $X_2$ , where*

the sliding window sizes are defined using time lags  $\tau_1 = \frac{2\pi}{w_{21}(M+1)}$  and  $\tau_2 = \frac{2\pi}{w_{22}(M+1)}$ , respectively. Similarly, define the 1D persistence diagrams from the VR filtrations on  $X_1$  and  $X_2$  as  $\text{dgm}_1(X_1)$  and  $\text{dgm}_1(X_2)$ , respectively. Let the max 1D persistence in each diagram be denoted by  $\text{mp}(\text{dgm}_1(X_1))$  and  $\text{mp}(\text{dgm}_1(X_2))$ , and the resulting conditional periodicity scores of  $f_1$  given  $f_{21}$  and  $f_1$  given  $f_{22}$  be denoted by  $\text{score}(f_1|f_{21})$  and  $\text{score}(f_1|f_{22})$ , respectively. Then the following results hold:

$$d_H(X_1, X_2) \leq \sqrt{M+1} \left| \frac{2\pi}{w_{21}} - \frac{2\pi}{w_{22}} \right| \sqrt{\sum_{i=2}^{M+1} |f'_1(c_i)|^2} \quad (2)$$

$$d_B(\text{dgm}_1(X_1), \text{dgm}_1(X_2)) \leq 2\sqrt{M+1} \left| \frac{2\pi}{w_{21}} - \frac{2\pi}{w_{22}} \right| \sqrt{\sum_{i=2}^{M+1} |f'_1(c_i)|^2} \quad (3)$$

$$|\text{mp}(\text{dgm}_1(X_1)) - \text{mp}(\text{dgm}_1(X_2))| \leq 4\sqrt{M+1} \left| \frac{2\pi}{w_{21}} - \frac{2\pi}{w_{22}} \right| \sqrt{\sum_{i=2}^{M+1} |f'_1(c_i)|^2} \quad (4)$$

$$|\text{score}(f_1|f_{21}) - \text{score}(f_1|f_{22})| \leq 4\sqrt{\frac{M+1}{3}} \left| \frac{2\pi}{w_{21}} - \frac{2\pi}{w_{22}} \right| \sqrt{\sum_{i=2}^{M+1} |f'_1(c_i)|^2} \quad (5)$$

for some  $c_i \in (t + i\tau_2, t + i\tau_1)$  and  $i = 1, \dots, M+1$ .

*Proof.* Bound on Hausdorff distance in Equation (2):

We first find an upper bound on the Euclidean distance between respective pairs of points in  $X_1$  and  $X_2$ , and then use it to find an upper bound on the Hausdorff distance between the two point clouds. Similar to the proof of Proposition 3.1, there exists some  $c_i \in (t + (i-1)\tau_2, t + (i-1)\tau_1)$  where

$$\begin{aligned} \|\text{SW}_{M,\tau} f_{1|21}(t) - \text{SW}_{M,\tau} f_{1|22}(t)\|_2 &= \left( \sum_{i=2}^{M+1} |f'_1(c_i)|^2 \left| \frac{i-1}{M+1} \right|^2 \left| \frac{2\pi}{w_{21}} - \frac{2\pi}{w_{22}} \right|^2 \right)^{\frac{1}{2}} \\ &\leq \frac{1}{M+1} \left| \frac{2\pi}{w_{21}} - \frac{2\pi}{w_{22}} \right| \sqrt{\sum_{i=2}^{M+1} |f'_1(c_i)|^2} \sqrt{\sum_{i=2}^{M+1} |i-1|} \\ &\quad \text{(by Cauchy-Schwartz inequality)} \\ &< \sqrt{M+1} \left| \frac{2\pi}{w_{21}} - \frac{2\pi}{w_{22}} \right| \sqrt{\sum_{i=2}^{M+1} |f'_1(c_i)|^2}. \end{aligned}$$

Let  $\epsilon > \sqrt{M+1} \left| \frac{2\pi}{w_{21}} - \frac{2\pi}{w_{22}} \right| \sqrt{\sum_{i=2}^{M+1} |f'_1(c_i)|^2}$ . Then  $X_1 \subset X_2^\epsilon$  and  $X_2 \subset X_1^\epsilon$ , so by Definition

2.1,  $d_H(X_1, X_2) \leq \epsilon$ . Taking the infimum of both sides yields the relation

$$d_H(X_1, X_2) \leq \sqrt{M+1} \left| \frac{2\pi}{w_{21}} - \frac{2\pi}{w_{22}} \right| \sqrt{\sum_{i=2}^{M+1} |f'_1(c_i)|^2}.$$

Bound on bottleneck distance in Equation (3):

By the bound on stability of persistence diagrams in Equation (1), we have that  $d_B(dgm_1(X_1), dgm_1(X_2)) \leq 2 d_H(X_1, X_2)$ , since  $X_1$  and  $X_2$  both lay in  $\mathbb{R}^{M+1}$ .

Bound on max persistence in Equation (4):

This proof is motivated by a similar result obtained for difference in the max persistence between embeddings of time series and their truncated Fourier approximations by Perea and Harer [19, Theorem 4.5 (2)]. Let  $(b_1^{\max}, d_1^{\max})$  and  $(b_2^{\max}, d_2^{\max})$  be the points corresponding to the 1D-features of max persistence in  $dgm_1(X_1)$  and  $dgm_1(X_2)$ , respectively. Let  $\epsilon^* = d_B(dgm_1(X_1), dgm_1(X_2))$ . Then by Definition 2.4, any pairs of points  $(b_1, d_1)$  and  $(b_2, d_2)$  in the respective diagrams satisfy  $\|(b_1, d_1) - (b_2, d_2)\|_\infty = \sup \{|b_1 - b_2|, |d_1 - d_2|\} \leq \epsilon^*$ . Hence,  $|b_1^{\max} - b_2^{\max}| \leq \epsilon^*$  and  $|d_1^{\max} - d_2^{\max}| \leq \epsilon^*$ . Therefore

$$|\text{mp}(dgm_1(X_1)) - \text{mp}(dgm_1(X_2))| \leq |d_1^{\max} - d_2^{\max}| + |b_1^{\max} - b_2^{\max}| \leq 2 d_B(dgm_1(X_1), dgm_1(X_2)).$$

Bound on the score in Equation (5): By Definition 2.7,

$$\begin{aligned} |\text{score}(f_1|f_{21}) - \text{score}(f_1|f_{22})| &= \frac{1}{\sqrt{3}} |\text{mp}(dgm_1(X_1)) - \text{mp}(dgm_1(X_2))| \\ &\leq \frac{2}{\sqrt{3}} d_B(dgm_1(X_1), dgm_1(X_2)) \\ &\leq \frac{4}{\sqrt{3}} d_H(X_1, X_2) \\ &\leq 4 \sqrt{\frac{M+1}{3}} \left| \frac{2\pi}{w_{21}} - \frac{2\pi}{w_{22}} \right| \sqrt{\sum_{i=2}^{M+1} |f'_1(c_i)|^2}. \end{aligned} \quad \square$$

We now derive lower bounds on the likelihood that our conditional periodicity score is stable under small amounts of Gaussian noise in  $f_1$  and  $f_2$ .

**Lemma 3.3** (Stability of score under added Gaussian noise). *Let  $f_1, f_2 : [0, 2\pi] \rightarrow \mathbb{R}$  be continuous, real-periodic time series. Let  $\sigma > 0$  denote the standard deviation of added Gaussian noise to  $f_1$ . Consider*

$$f_1^\sigma(t) = f_1(t) + \epsilon_t,$$

where  $\epsilon_t \sim N(0, \sigma^2)$  is a randomly sampled scalar from the associated Gaussian distribution. Define the constant  $a = \frac{\sigma}{\sqrt{\delta}}$  for some  $\delta \in (0, 1)$ . Denote the conditional periodicity score under this added noise at  $\sigma$  by  $\text{score}_\sigma(f_1|f_2)$ . Then it is at least  $(1 - \delta) \cdot 100\%$  likely that

$$|\text{score}(f_1|f_2) - \text{score}_\sigma(f_1|f_2)| \leq 4\sigma \sqrt{\frac{M+1}{3\delta}}.$$

*Proof.* Define the time series  $f_1$  at noise level  $\sigma$  by  $f_1^\sigma(t) = f_1(t) + \epsilon_t$  for  $\epsilon_t \sim N(0, \sigma^2)$ . Then the conditional embedding at noise level  $\sigma$  is denoted

$$\begin{aligned} \text{SW}_{M,\tau}^\sigma f_{1|2}(t) &= \left( f_1^\sigma(t), f_1^\sigma(t + \tau), \dots, f_1^\sigma(t + M\tau) \right)^T \\ &= \left( f_1(t) + \epsilon_t, f_1(t + \tau) + \epsilon_{t+\tau}, \dots, f_1(t + M\tau) + \epsilon_{t+M\tau} \right)^T. \end{aligned}$$

By our assumption, we have that  $\delta = \left(\frac{\sigma}{a}\right)^2$ . By Chebyshev's inequality, the probability that any given draw  $\epsilon_t$  deviates from the mean of zero by at least  $a$  is given by  $P[|\epsilon_t| \geq a] \leq \delta$ . Hence, the probability that  $\epsilon_t$  is within  $a$  of the mean is given by  $P[|\epsilon_t| \leq a] \geq 1 - \delta$ . Put another way, it is at least  $(1 - \delta) \cdot 100\%$  likely that  $|\epsilon_t| \leq a$ . Hence

$$\begin{aligned} \left\| \text{SW}_{M,\tau} f_{1|2}(t) - \text{SW}_{M,\tau}^\sigma f_{1|2}(t) \right\|_2 &= \sqrt{\sum_{i=1}^{M+1} |\epsilon_{t+(i-1)\tau}|^2} \\ &\leq a\sqrt{M+1} \quad \text{with at least } (1 - \delta) \cdot 100\% \text{ likelihood.} \end{aligned}$$

Hence, by similar arguments as in the proof of Theorem 3.2, it is at least  $(1 - \delta) \cdot 100\%$  likely that

$$|\text{score}(f_1|f_2) - \text{score}_\sigma(f_1|f_2)| \leq \frac{4a\sqrt{M+1}}{\sqrt{3}} = 4\sigma\sqrt{\frac{M+1}{3\delta}}. \quad \square$$

### 3.1 Stability of Score under PCA

The main bottleneck when using the periodicity score in practice is the computation of the dimension 1 persistence diagram of the Vietoris-Rips filtration of the SWE. In general, for a point cloud  $X$  with  $N$  points, the computation of  $\text{dgm}_1(X)$  runs in  $O(N^6)$  time, although faster approaches may be available in lower dimensions [14]. Moreover, in Theorem 3.6 below we prove that greater precision of  $\text{score}(f_1|f_2)$  warrants larger embedding dimensions. For sufficiently large enough embedding dimensions (i.e.  $M > 10$ ), pairwise Euclidean distances used to compute VR-complexes during filtration start to converge [2]. This could lead to inaccurate topological summaries when computing  $\text{score}(f_1|f_2)$ . As such, we study the conditional periodicity score under principal component analysis (PCA), a widely used dimension reduction technique [12].

**Theorem 3.4** (Stability of Conditional Periodicity Score Under PCA). *Let  $K \leq M+1$  for  $K \in \mathbb{N}$ . Suppose  $f_2$  is more periodic than  $f_1$  on  $[0, 2\pi]$  with cycle lengths  $\frac{2\pi}{w_2} \leq \frac{2\pi}{w_1}$ , respectively. For  $T = \left[0, \frac{2\pi}{w_1}\right]$ , define the orthogonal projection of  $X = \text{SW}_{M,\tau} f_{1|2}(T)$  onto its top  $K$  principal components by  $\phi(X) = (\langle \mathbf{c}_1, X \rangle, \dots, \langle \mathbf{c}_K, X \rangle)^T$  for orthonormal eigenvectors and corresponding eigenvalues  $\{\mathbf{c}_k, \lambda_k\}_{k=1}^N$  produced by PCA. Suppose  $X$  contains  $N \in \mathbb{N}$  points. Denote the conditional periodicity score under  $\phi$ ,  $\text{score}_\phi(f_1|f_2)$ , as the maximum 1-d persistence from the VR-filtration on  $\phi(X)$  divided by  $\sqrt{3}$ . Then*

$$|\text{score}(f_1|f_2) - \text{score}_\phi(f_1|f_2)| \leq \sqrt{\frac{8}{3}} \sqrt[4]{\sum_{i=K+1}^N \lambda_i^2}.$$

*Proof.* Our proof is inspired by methods used in [17]. Notice that  $\phi$  is a relation in  $\mathcal{R}(X, Y)$  for  $Y = \phi(X)$ . Then by Definition 2.3 we have that  $d_{\text{GH}}(X, Y) \leq \frac{1}{2} \text{dis}(\phi)$ , where  $\text{dis}(\phi)^2 = \|D_X - D_Y\|_{\max}^2$  with  $D_X$  being the matrix of pairwise distances in  $X$ . We get that [17, Lemma 3.9]

$$\|D_X - D_Y\|_{\max}^2 \leq \left\| D_X^{\circ 2} - D_Y^{\circ 2} \right\|_{\max},$$

where  $D_X^{\circ 2}$  denotes the matrix of squared pairwise Euclidean distances in  $X$ .

Recall that for a matrix  $A$ ,  $\|A\|_{\max}^2 = (\max_{ij} |A_{ij}|)^2 = \max_{ij} |A_{ij}|^2 \leq \sum_{ij} |A_{ij}|^2 = \|A\|_F^2$ ,

where  $\|\cdot\|_F$  denotes the Frobenius norm. Then we have

$$\left\| D_X^{\circ 2} - D_Y^{\circ 2} \right\|_{\max} \leq \left\| D_X^{\circ 2} - D_Y^{\circ 2} \right\|_F.$$

Define the eigendecomposition of the covariance of  $X$  as  $XX^T = Q\Lambda Q^T$ , where  $Q = [\mathbf{c}_1, \dots, \mathbf{c}_N]$  is the  $N \times N$  matrix of orthonormal eigenvectors and  $\Lambda = \text{diag}(\lambda_1, \dots, \lambda_N)$  is the  $N \times N$  diagonal matrix of eigenvalues corresponding to the orthogonal projection of  $X$ . Then the eigendecomposition of the  $K$ -dimensional subspace containing the top  $K$  principal components of  $X$  can be defined by  $YY^T = Q\Lambda|_K Q^T$ , where  $\Lambda|_K = \text{diag}(\lambda_1, \dots, \lambda_K, \underbrace{0, \dots, 0}_{N-K})$ . Then, if we center the

squared distances in  $D_X^{\circ 2}$  and  $D_Y^{\circ 2}$ , we obtain the relations [3]

$$\begin{aligned} XX^T &= -\frac{1}{2}C_N D_X^{\circ 2} C_N \text{ and} \\ YY^T &= -\frac{1}{2}C_N D_Y^{\circ 2} C_N, \end{aligned}$$

where  $C_N$  is the  $N \times N$  centering matrix with diagonal entries  $1 - \frac{1}{N}$  and off-diagonal entries  $-\frac{1}{N}$ . Then  $D_X^{\circ 2} = -2C_N(Q\Lambda Q^T)C_N$  and  $D_Y^{\circ 2} = -2C_N(Q\Lambda|_K Q^T)C_N$ . Since  $Q^T Q = Q Q^T = I$ , we obtain that

$$\begin{aligned} \left\| D_X^{\circ 2} - D_Y^{\circ 2} \right\|_F &= 2 \left\| C_N(Q\Lambda Q^T - Q\Lambda|_K Q^T)C_N \right\|_F \\ &= 2 \left\| Q(\Lambda - \Lambda|_K)Q^T \right\|_F \quad (\text{since } C_N \approx I \text{ for sufficiently large } N) \\ &= 2\sqrt{\text{tr}(Q(\Lambda - \Lambda|_K)^2 Q^T)} \\ &= 2\sqrt{\text{tr}((\Lambda - \Lambda|_K)^2)} \quad (\text{since trace is cyclically invariant}) \\ &= 2\sqrt{\sum_{i=K+1}^N \lambda_i^2}. \end{aligned}$$

Thus we get that  $\text{dis}(\phi) \leq \sqrt{2} \sqrt[4]{\sum_{i=K+1}^N \lambda_i^2}$  and hence  $d_{\text{GH}}(X, Y) \leq \frac{\sqrt{2}}{2} \sqrt[4]{\sum_{i=K+1}^N \lambda_i^2}$ . Then again by

the standard result on stability of persistence diagrams (Equation (1)), we get that

$$d_B(dgm_1(X), dgm_1(Y)) \leq 2 d_{GH}(X, Y) \leq \sqrt{2} \sqrt[4]{\sum_{i=K+1}^N \lambda_i^2}.$$

Hence by similar arguments to those in the proof of Theorem 3.2, we have that

$$\begin{aligned} |\text{score}(f_1|f_2) - \text{score}_\phi(f_1|f_2)| &= \frac{1}{\sqrt{3}} |\text{mp}(dgm_1(X)) - \text{mp}(dgm_1(\phi(X)))| \\ &\leq \frac{2}{\sqrt{3}} d_B(dgm_1(X), dgm_1(\phi(X))) \\ &\leq 2 \sqrt{\frac{2}{3}} \sqrt[4]{\sum_{i=K+1}^N \lambda_i^2}. \\ &= \sqrt{\frac{8}{3}} \sqrt[4]{\sum_{i=K+1}^N \lambda_i^2}. \end{aligned} \quad \square$$

Theorem 3.4 shows that if the top  $K$  principal components of the conditional SWE capture most of its structure, then the conditional periodicity score will not change much under the associated orthogonal projection. We now reveal a direct consequence of this stability under small changes in periodicity of  $f_2$ .

**Corollary 3.5** (Consequence of Stability of Conditional Periodicity Score Under PCA). *Let  $K \leq M + 1$  for  $K \in \mathbb{N}$ . Suppose  $f_2$  is more periodic than  $f_1$  on  $[0, 2\pi]$  with cycle lengths  $\frac{2\pi}{w_2} \leq \frac{2\pi}{w_1}$ , respectively. For  $T = \left[0, \frac{2\pi}{w_1}\right]$ , define the orthogonal projections of  $X_1 = \text{SW}_{M, \tau_1} f_{1|2}(T)$  and  $X_2 = \text{SW}_{M, \tau_2} f_{1|2}(T)$  onto their top  $K$  principal components by the relations  $\phi_1(X_1) = (\langle \mathbf{c}_1, X_1 \rangle, \dots, \langle \mathbf{c}_K, X_1 \rangle)^T$  and  $\phi_2(X_2) = (\langle \mathbf{d}_1, X_2 \rangle, \dots, \langle \mathbf{d}_K, X_2 \rangle)^T$  for orthonormal eigenvectors and corresponding eigenvalues  $\{\mathbf{c}_k, \lambda_k\}_{k=1}^N, \{\mathbf{d}_k, \gamma_k\}_{k=1}^N$  produced by PCA. Suppose  $X_1$  and  $X_2$  each contain  $N \in \mathbb{N}$  points. Define the conditional periodicity score of  $f_1$  given  $f_{21}$  and  $f_1$  given  $f_{22}$  under  $\phi_1$  and  $\phi_2$ , respectively, as  $\text{score}_{\phi_1}(f_1|f_{21})$  and  $\text{score}_{\phi_2}(f_1|f_{22})$ . Then the following inequality holds:*

$$\begin{aligned} |\text{score}_{\phi_1}(f_1|f_{21}) - \text{score}_{\phi_2}(f_1|f_{22})| &\leq \sqrt{\frac{8}{3}} \left( \sqrt[4]{\sum_{i=K+1}^N \lambda_i^2} + \sqrt[4]{\sum_{i=K+1}^N \gamma_i^2} \right) \\ &\quad + |\text{score}(f_1|f_{21}) - \text{score}(f_1|f_{22})|. \end{aligned}$$

*Proof.* By Theorem 3.4, we have that

$$|\text{score}_{\phi_1}(f_1|f_{21}) - \text{score}(f_1|f_{21})| \leq \sqrt{\frac{8}{3}} \sqrt[4]{\sum_{i=K+1}^N \lambda_i^2} \quad \text{and}$$

$$|\text{score}_{\phi_2}(f_1|f_{22}) - \text{score}(f_1|f_{22})| \leq \sqrt{\frac{8}{3}} \sqrt[4]{\sum_{i=K+1}^N \gamma_i^2}.$$

Hence we get

$$\begin{aligned} & |\text{score}_{\phi_1}(f_1|f_{21}) - \text{score}_{\phi_2}(f_1|f_{21})| \\ & \leq |\text{score}_{\phi_1}(f_1|f_{21}) - \text{score}(f_1|f_{21})| + |\text{score}(f_1|f_{21}) - \text{score}(f_1|f_{22})| \\ & \quad + |\text{score}(f_1|f_{22}) - \text{score}_{\phi_2}(f_1|f_{22})| \\ & \leq \sqrt{\frac{8}{3}} \left( \sqrt[4]{\sum_{i=K+1}^N \lambda_i^2} + \sqrt[4]{\sum_{i=K+1}^N \gamma_i^2} \right) + |\text{score}(f_1|f_{21}) - \text{score}(f_1|f_{22})|. \end{aligned} \quad \square$$

Corollary 3.5 reveals that small changes in periodicity of  $f_2$  still yield small changes in the  $\text{score}(f_1|f_2)$  under orthogonal projection if the top  $K$  principal components of the conditional SWE capture most of its structure.

## 3.2 A Minimum Embedding Dimension for Convergence

We define a minimum embedding dimension  $\mathcal{M}$  that we can use to control the convergence behavior of the conditional periodicity score at dimension  $M \in \mathbb{N}$ , denoted  $\text{score}_M(f_1|f_2)$ , near the limiting score,  $\text{score}(f_1|f_2)$ .

**Theorem 3.6** (Minimum embedding dimension for convergence). *Let  $\epsilon > 0$ . Suppose  $f_2$  is more periodic than  $f_1$  on  $T = [0, 2\pi]$  with cycle lengths  $\frac{2\pi}{w_2} \leq \frac{2\pi}{w_1}$ , respectively. Then, any embedding dimension  $M_2 > M_1 \geq \mathcal{M} \in \mathbb{N}$  for  $\mathcal{M} = \left\lceil \frac{2\pi}{w_2 \epsilon} \right\rceil$  guarantees that the change in respective conditional periodicity scores  $\text{score}_{M_2}(f_1|f_2)$  and  $\text{score}_{M_1}(f_1|f_2)$  are linearly bounded above by  $\epsilon$ .*

*Proof.* We first show that  $\tau = \frac{2\pi}{w_2(M+1)}$  is a Cauchy sequence of  $M$ . By the definition of  $\mathcal{M}$ ,  $\mathcal{M} \geq \frac{2\pi}{w_2 \epsilon}$  and hence  $\frac{2\pi}{w_2 \mathcal{M}} \leq \epsilon \implies \frac{2\pi}{w_2} \left( \frac{1}{\mathcal{M}} \right) \leq \epsilon$ . Since  $M_2 > M_1 \geq \mathcal{M}$ ,  $M_2 + 1 > M_1 + 1 \geq \mathcal{M} + 1$  and hence  $\frac{1}{M_2 + 1} < \frac{1}{M_1 + 1} \leq \frac{1}{\mathcal{M} + 1} < \frac{1}{\mathcal{M}}$ . Thus we get

$$\begin{aligned} |\tau(M_1) - \tau(M_2)| &= \frac{2\pi}{w_2} \left| \frac{1}{M_1 + 1} - \frac{1}{M_2 + 1} \right| \\ &= \frac{2\pi}{w_2} \left( \frac{1}{M_1 + 1} - \frac{1}{M_2 + 1} \right) \\ &\leq \frac{2\pi}{w_2} \left( \frac{1}{\mathcal{M} + 1} - \frac{1}{M_2 + 1} \right) \\ &< \frac{2\pi}{w_2} \left( \frac{1}{\mathcal{M}} \right) \leq \epsilon. \end{aligned} \quad (6)$$

Define the zero-padded conditional SWE of  $f_1$  given  $f_2$  for the smaller embedding dimension  $M_1$  by  $\text{SW}_{M_1, \tau(M_1)} f_{1|2}(t) = \left( f_1(t), \dots, f_1(t + M_1 \tau(M_1)), \underbrace{0, \dots, 0}_{M_2 - M_1} \right)^T$ . Then for  $i = 1, \dots, M_1 + 1$ , by the MVT there exists some  $c_i \in I_i = \left( t + (i-1)\tau(M_2), t + (i-1)\tau(M_1) \right)$  such that

$$|f'_1(c_i)| \left| (i-1) \left( \tau(M_1) - \tau(M_2) \right) \right| = \left| f_1(t + (i-1)\tau(M_1)) - f_1(t + (i-1)\tau(M_2)) \right|. \quad (7)$$

Applying the results in Equations (6) and (7), we obtain the following relation.

$$\begin{aligned} & \left\| \text{SW}_{M_1, \tau(M_1)} f_{1|2}(t) - \text{SW}_{M_2, \tau(M_2)} f_{1|2}(t) \right\|_2^2 \\ &= \sum_{i=1}^{M_1+1} \left| f_1 \left( t + (i-1)\tau(M_1) \right) - f_1 \left( t + (i-1)\tau(M_2) \right) \right|^2 + \sum_{M_1+1}^{M_2+1} \left| f_1 \left( t + (i-1)\tau(M_2) \right) \right|^2 \\ &= \sum_{i=1}^{M_1+1} |f'_1(c_i)|^2 |i-1|^2 |\tau(M_1) - \tau(M_2)|^2 + \sum_{M_1+1}^{M_2+1} \left| f_1 \left( t + (i-1)\tau(M_2) \right) \right|^2 \\ &\leq \epsilon^2 (M_1 + 1)^3 \sqrt{\sum_{i=1}^{M_1+1} |f'_1(c_i)|^2} + \sum_{M_1+1}^{M_2+1} \left| f_1 \left( t + (i-1)\tau(M_2) \right) \right|^2 \\ &= \epsilon^2 \cdot g(M_1, f_1) + h(M_1, M_2, f_1) \\ &\leq \left( \epsilon \cdot \sqrt{g(M_1, f_1)} + \sqrt{h(M_1, M_2, f_1)} \right)^2, \end{aligned}$$

since  $g(M_1, f_1)$  and  $h(M_1, M_2, f_1)$  are nonnegative constants for any given comparison, and  $\epsilon > 0$ .

$$\text{Then } d_H \left( \text{SW}_{M_1, \tau(M_1)} f_{1|2}(t), \text{SW}_{M_2, \tau(M_2)} f_{1|2}(t) \right) \leq \epsilon \cdot \sqrt{g(M_1, f_1)} + \sqrt{h(M_1, M_2, f_1)},$$

which implies that

$$d_B \left( \text{dgm}_1(\text{SW}_{M_1, \tau(M_1)} f_{1|2}(t)), \text{dgm}_1(\text{SW}_{M_2, \tau(M_2)} f_{1|2}(t)) \right) \leq \epsilon \cdot 2\sqrt{g(M_1, f_1)} + 2\sqrt{h(M_1, M_2, f_1)}.$$

By a similar argument as in the proof of Theorem 3.2 (Equation (3)), this means that

$$\begin{aligned} & \left| \text{mp} \left( \text{dgm}_1(\text{SW}_{M_1, \tau(M_1)} f_{1|2}(t)) \right) - \text{mp} \left( \text{dgm}_1(\text{SW}_{M_2, \tau(M_2)} f_{1|2}(t)) \right) \right| \\ & \leq \epsilon \cdot 4\sqrt{g(M_1, f_1)} + 4\sqrt{h(M_1, M_2, f_1)} \\ \implies & | \text{score}_{M_1}(f_1|f_2) - \text{score}_{M_2}(f_1|f_2) | \leq \frac{4}{\sqrt{3}} \left( \epsilon \cdot \sqrt{g(M_1, f_1)} + \sqrt{h(M_1, M_2, f_1)} \right). \end{aligned}$$

Hence the difference between the scores under  $M_1$  and  $M_2$  is bounded above by a linear function of  $\epsilon$  with positive slope. Therefore, the smaller the  $\epsilon$ -precision is, the closer these scores are to each other.  $\square$

Theorem 3.6 tells us that the time lag is a Cauchy sequence of the embedding dimension, where smaller values of  $\epsilon$  yield larger input embedding dimensions which increase the precision of convergence of  $\text{score}_M(f_1|f_2)$  to  $\text{score}(f_1|f_2)$ . In other words, the greater the precision of convergence wanted, the smaller the value of  $\epsilon$  we must choose, the greater the minimum embedding dimension required, and the closer the conditional periodicity scores for any pair of higher-valued dimensions will be. This result can be useful if we want to ensure that the conditional scores we are computing for a given input dimension  $M$  are similar to the underlying conditional periodicity score, albeit at the cost of higher run times and more embedding points required due to a larger embedding dimension. We next prove that small changes in  $\epsilon$  induce small changes in minimum embedding dimension  $\mathcal{M}$ .

**Corollary 3.7** (Stability of Minimum Embedding Dimension). *Let  $f_1, f_2 : [0, 2\pi] \rightarrow \mathbb{R}$  be  $w_1$ - and  $w_2$ -periodic time series such that  $w_2 > w_1$ . Let  $\epsilon > 0$  and fix the minimum embedding dimension for  $\text{score}(f_1|f_2)$  to  $M(\epsilon) = \mathcal{M}$  as specified in Theorem 3.6. Without loss of generality, let  $\epsilon_1 > \epsilon_2 > 0$ . Then for some  $c \in (\epsilon_2, \epsilon_1)$ , we have*

$$|M(\epsilon_1) - M(\epsilon_2)| \leq \frac{2\pi}{w_2} \cdot \frac{1}{c^2} \cdot |\epsilon_1 - \epsilon_2| + 2.$$

*Proof.* By the Triangle inequality,

$$|M(\epsilon_1) - M(\epsilon_2)| \leq \left| \left\lceil \frac{2\pi}{w_2\epsilon_1} \right\rceil - \frac{2\pi}{w_2\epsilon_1} \right| + \left| \frac{2\pi}{w_1\epsilon_1} - \frac{2\pi}{w_2\epsilon_2} \right| + \left| \frac{2\pi}{w_2\epsilon_2} - \left\lceil \frac{2\pi}{w_2\epsilon_2} \right\rceil \right|.$$

Since  $\left\lceil \frac{2\pi}{w_2\epsilon} \right\rceil \leq \frac{2\pi}{w_2\epsilon} \leq \left\lceil \frac{2\pi}{w_2\epsilon} \right\rceil$ , the distance  $\left| \frac{2\pi}{w_2\epsilon} - \left\lceil \frac{2\pi}{w_2\epsilon} \right\rceil \right|$  is at most 1. Hence,

$$|M(\epsilon_1) - M(\epsilon_2)| \leq \left| \frac{2\pi}{w_2\epsilon_1} - \frac{2\pi}{w_2\epsilon_2} \right| + 2.$$

Let  $f(\epsilon) = \frac{1}{\epsilon}$ . Then  $f'(\epsilon) = -\frac{1}{\epsilon^2}$  and by MVT there exists some  $c \in (\epsilon_2, \epsilon_1)$  such that

$$\left| \frac{1}{\epsilon_1} - \frac{1}{\epsilon_2} \right| = \frac{1}{c^2} |\epsilon_1 - \epsilon_2|.$$

Combining the above two expressions gives

$$|M(\epsilon_1) - M(\epsilon_2)| \leq \frac{2\pi}{w_2} \left| \frac{1}{\epsilon_1} - \frac{1}{\epsilon_2} \right| + 2 \leq \frac{2\pi}{w_2} \cdot \frac{1}{c^2} \cdot |\epsilon_1 - \epsilon_2| + 2. \quad \square$$

Corollary 3.7 ensures that small changes in the desired precision  $\epsilon$  of  $\text{score}(f_1|f_2)$  induce small changes in minimum embedding dimension  $\mathcal{M}$ . Intuitively, greater desired precision induces smaller distances  $|\epsilon_1 - \epsilon_2|$  and  $c \in (\epsilon_2, \epsilon_1)$ , and hence yields smaller changes in  $\mathcal{M}$ . Oppositely, less desired precision increases  $|\epsilon_1 - \epsilon_2|$  and  $c$ , and hence produces larger changes in  $\mathcal{M}$ .

**Proposition 3.8** (A minimum number of embedding points). *Let  $f_1, f_2 : T \subset [0, 2\pi] \rightarrow \mathbb{R}$  be two discrete univariate time series on  $[0, 2\pi]$ . Suppose  $\frac{2\pi}{w_2} < \frac{2\pi}{w_1}$  for  $w_1, w_2 \in \mathbb{N}$ . Let  $T =$*

$\{t_0 = 0 < t_1 < \dots < t_P = 2\pi\}$  for  $P \in \mathbb{N}$ . Let  $M = M_1 \in \mathbb{N}$ . Suppose there exists  $\delta \in \mathbb{N}$  points in  $\left[0, \frac{\pi}{w_2}\right]$ . Then the minimum number of embedding points  $N \in \mathbb{N}$  required to capture the relationship between the periodicities of  $f_1$  and  $f_2$  in the conditional SWE satisfies

$$N \geq \frac{P}{w_1} - \delta.$$

*Proof.* Let  $M = M_1 \in \mathbb{N}$ . Suppose there exists  $\delta_1 < P$  points on  $[0, M_1\tau]$  for  $M_1\tau = \frac{2\pi}{w_2} \cdot \frac{M_1}{(M_1 + \tau)}$ . Then there exists  $\frac{P}{w_1} - \delta_1$  points in  $\text{SW}_{M_1, \tau} f_{1|2}([0, M_1\tau])$ . Suppose we increase  $M$  to  $M_2 > M_1$ . Then there exists  $\delta_2 > \delta_1$  points on  $[0, M_2\tau]$ , since

$$M_2\tau = \frac{2\pi}{w_2} \cdot \frac{M_2}{(M_2 + 1)} > \frac{2\pi}{w_2} \cdot \frac{M_1}{(M_1 + 1)} = M_1\tau.$$

Hence, there exists  $\frac{P}{w_1} - \delta_2 < \frac{P}{w_1} - \delta_1$  points in  $\text{SW}_{M_2, \tau} f_{1|2}([0, M_2\tau])$ , since  $\delta_2 > \delta_1$ . Therefore, increasing  $M$  decreases the number of points in the conditional SWE. Hence, to maximize the number of points in  $\text{SW}_{M, \tau} f_{1|2}(T)$ ,  $N$ , we must let  $N \geq \frac{P}{w_1} - \delta_1$ . The smallest such  $\delta$  occurs when  $M = 1$ , since any larger dimension increases  $[0, M\tau]$  and thus decreases  $\frac{P}{w_1} - \delta$ . Therefore, we let

$$N \geq \frac{P}{w_1} - \delta,$$

where  $\delta$  is the number of points in  $[0, \tau] = \left[0, \frac{\pi}{w_2}\right]$ .  $\square$

### 3.3 Stability versus Convergence of $\text{score}(f_2|f_2)$

We highlight the difference between the stability and convergence results we have proven. The main difference is that although small changes in periodicity of  $f_2$  and Gaussian noise in  $f_1$  guarantee small changes in  $\text{score}(f_1|f_2)$  (Theorem 3.2 and Proposition 3.3), this does not necessarily guarantee that the conditional scores computed are close to the underlying score. This closeness (i.e., convergence) is guaranteed whenever  $M = \mathcal{M} = \left\lceil \frac{2\pi}{w_2\epsilon} \right\rceil$ , as proven in Theorem 3.6. We show an example of this main difference in Figure 4, where we can see that although increased embedding dimensions may produce larger changes in the conditional periodicity score, this score remains closer to the underlying score when we choose  $M = \mathcal{M}$ .

## 4 Computational Results

We present a framework for computing the conditional periodicity score using PCA. We then apply this framework on periodic signals of multiple types. We also compare the performance of our conditional periodicity score with that of percent determinism.

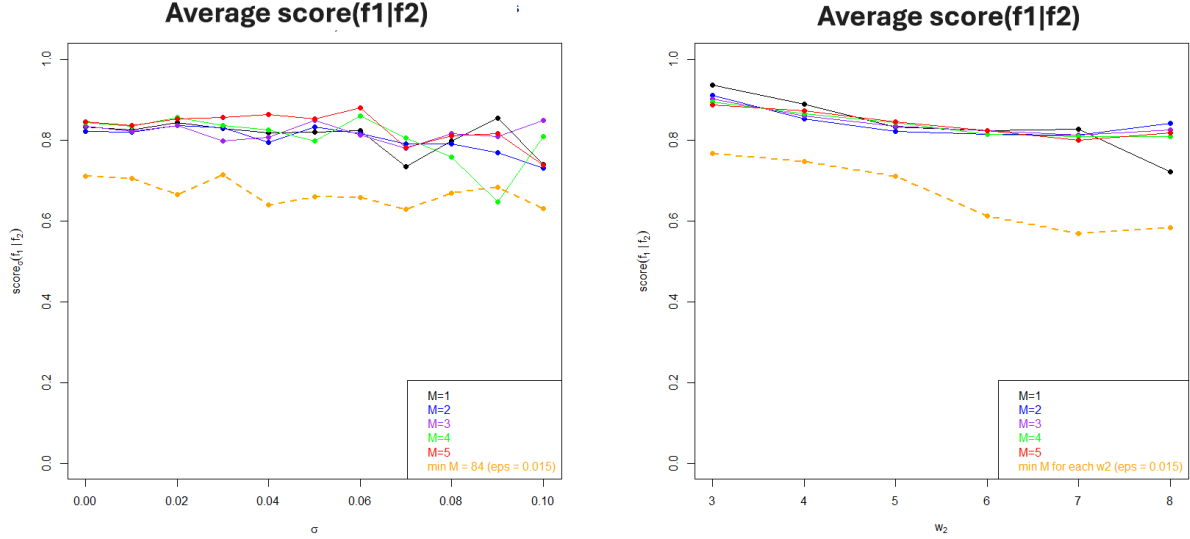


Figure 4: An example of the stability versus convergence behavior of the conditional periodicity score. The left image shows the stability of our score against small changes in Gaussian noise versus the increased ‘closeness’ of our score to the underlying score when  $M = \left\lceil \frac{2\pi}{w_2\epsilon} \right\rceil$ . The right image shows the same but for small changes in cycle length of  $f_2$ ,  $\frac{2\pi}{w_2}$ .

## 4.1 Procedure for Quantifying Conditional Periodicity

We introduce a procedure for computing the conditional periodicity score of a discrete time series  $\{f_i(t_p)\}_{p=1}^P$  given another  $\{f_j(t_p)\}_{p=1}^P$ ,  $P \in \mathbb{N}$  (see Algorithm 1). We first fit two continuous time series  $f_i^{\text{cts}}$  and  $f_j^{\text{cts}}$  onto each discrete signal over the interval  $[0, 2\pi]$  via cubic spline interpolation [20]. We then estimate the length of one cycle of  $f_i$  and  $f_j$  using the discrete fast Fourier transform (FFT) on the continuously-fitted series. More specifically, we compute the discrete fast Fourier spectra of  $f_i$  and  $f_j$  up to their Nyquist frequency of  $\frac{P}{2}$ . We then estimate  $w_i$  and  $w_j$  as the frequency indices corresponding to the maximum spectral densities corresponding to  $f_i$  and  $f_j$ , respectively. We assign  $f_1$  as the series with the larger cycle-length and  $f_2$  as that with the smaller length. We then compute the top  $K$  principal components of the conditional SWE.

Assuming the embedding dimension  $M + 1$  is at least 3, we choose  $K = 2$ . This is because, assuming we are working with  $L$ -periodic time series, such embeddings will be elliptic curves and hence we presume that 2 principal components will suffice. As an example to motivate our choice of  $K = 2$ , see Figure 5. In this example, we fix the periodicity of  $f_1$  so that  $w_1 = 3$ , the embedding dimension to  $M = 10$ , and increase the periodicity of  $f_2$  so that  $w_2$  varies from  $w_1$  to 15. We set the standard deviation of noise to  $\sigma = 0.15$ ,  $P = 300$  time points, the simple moving average (SMA) window size to 19 points, and  $N = \frac{P}{w_1} - 2 = 198$  (see Proposition 3.8). We compute the average variance captured by all principal components among 100 samples for each  $w_2$ . Notice that if  $w_2$  is close to  $w_1$ , then the conditional SWE is quite round, and hence two principal components capture roughly the same majority of variance in the data. If  $w_2$  is much larger than  $w_1$ , then the conditional

SWE is more “skinny” and hence two principal components should still capture a majority of the variance, but the first component will capture more than the second.

We finally perform VR filtration on the SWE, obtaining the conditional periodicity score termed  $\text{score}_\phi(\cdot)$  under the PCA projection  $\phi$ .

---

**Algorithm 1:** Procedure for quantifying conditional periodicity

---

**Inputs :** Embedding dimension  $M \in \mathbb{N}$ ,  $N \in \mathbb{N}$  points in the conditional SWE, and two discrete univariate time series  $f_i, f_j$  defined on  $\{t_1, \dots, t_P : P \in \mathbb{N}\}$ .

- 1 **Fit** a continuous signal  $f_k^{\text{cts}} : [0, 2\pi] \rightarrow \mathbb{R}$  to the discrete signal  $f_k$  via cubic spline interpolation such that  $f_k^{\text{cts}}(0) = f_k(t_1)$  and  $f_k^{\text{cts}}(2\pi) = f_k(t_P)$  for  $k = i, j$ .
- 2 **Estimate**  $\frac{2\pi}{w_i}$  and  $\frac{2\pi}{w_j}$  via spectral analysis using the (Discrete) Fast Fourier Transform. Assign  $f_1$  to be the less periodic and  $f_2$  to be the more periodic signal of the pair  $\{f_i^{\text{cts}}, f_j^{\text{cts}}\}$ . That is, define :

$$\frac{2\pi}{w_1} = \max \left\{ \frac{2\pi}{w_i}, \frac{2\pi}{w_j} \right\}, \quad \frac{2\pi}{w_2} = \min \left\{ \frac{2\pi}{w_i}, \frac{2\pi}{w_j} \right\}$$

$$f_1 = \left\{ f_k^{\text{cts}} : \frac{2\pi}{w_k} = \frac{2\pi}{w_1} \right\}, \quad f_2 = \left\{ f_k^{\text{cts}} : \frac{2\pi}{w_k} = \frac{2\pi}{w_2} \right\}$$

- 3 **Define**  $\tau = \frac{2\pi}{w_2(M+1)}$ .
- 4 **Compute**  $X = \text{SW}_{M,\tau} f_{1|2}(T)$  for  $N$  evenly-spaced time points in  $T = \left[0, \frac{2\pi}{w_1}\right]$ .
- 5 For  $K = \min\{2, M+1\}$ , compute  $\phi : \mathbb{R}^{M+1} \rightarrow \mathbb{R}^K$ , the orthogonal projection of  $X$  onto its first  $K$  principal components ( $K = 2$ , typically).
- 6 Center and normalize  $\phi(X)$  to obtain  $Y$ .
- 7 Compute  $\text{dgm}_1(Y)$  from VR filtration on  $Y$  and  $\text{mp}(\text{dgm}_1(Y))$  from  $\text{dgm}_1(Y)$ .
- 8 Compute  $\text{score}_\phi(f_1|f_2)$  using  $\text{mp}(\text{dgm}_1(Y))$ .

**Return:**  $\{\text{score}_\phi(f_1|f_2), w_1, w_2, f_i \text{ assignment}, f_j \text{ assignment}\}$ .

---

**Remark 4.1** (Computational Complexity of Conditional Periodicity Score). *Algorithm 1 runs in  $O(P \log P + NK^2 + N^6)$  time, where  $P$  is the number of points in the discrete univariate input signals  $f_i$  and  $f_j$ ,  $N$  is the number of points in the conditional SWE of the fitted continuous signals  $f_1$  given  $f_2$ , and  $K < M+1$  is the number of principal components used for the conditional SWE where  $M$  is the embedding dimension. We take  $K = 2$  by default. The cubic spline interpolation on  $f_i$  and  $f_j$  runs in  $O(P)$  time [11] and the discrete FFT on  $f_i^{\text{cts}}, f_j^{\text{cts}}$  can be computed in  $O(P \log P)$  time [4]. The PCA computations run in  $O(NK^2)$  time [12, 26]. The bottleneck step is usually the computation of the 1D persistence diagram using the VR filtration of  $Y$ , which runs in  $O(N^6)$  time [14].*

## Scree Plots for 15% Noise

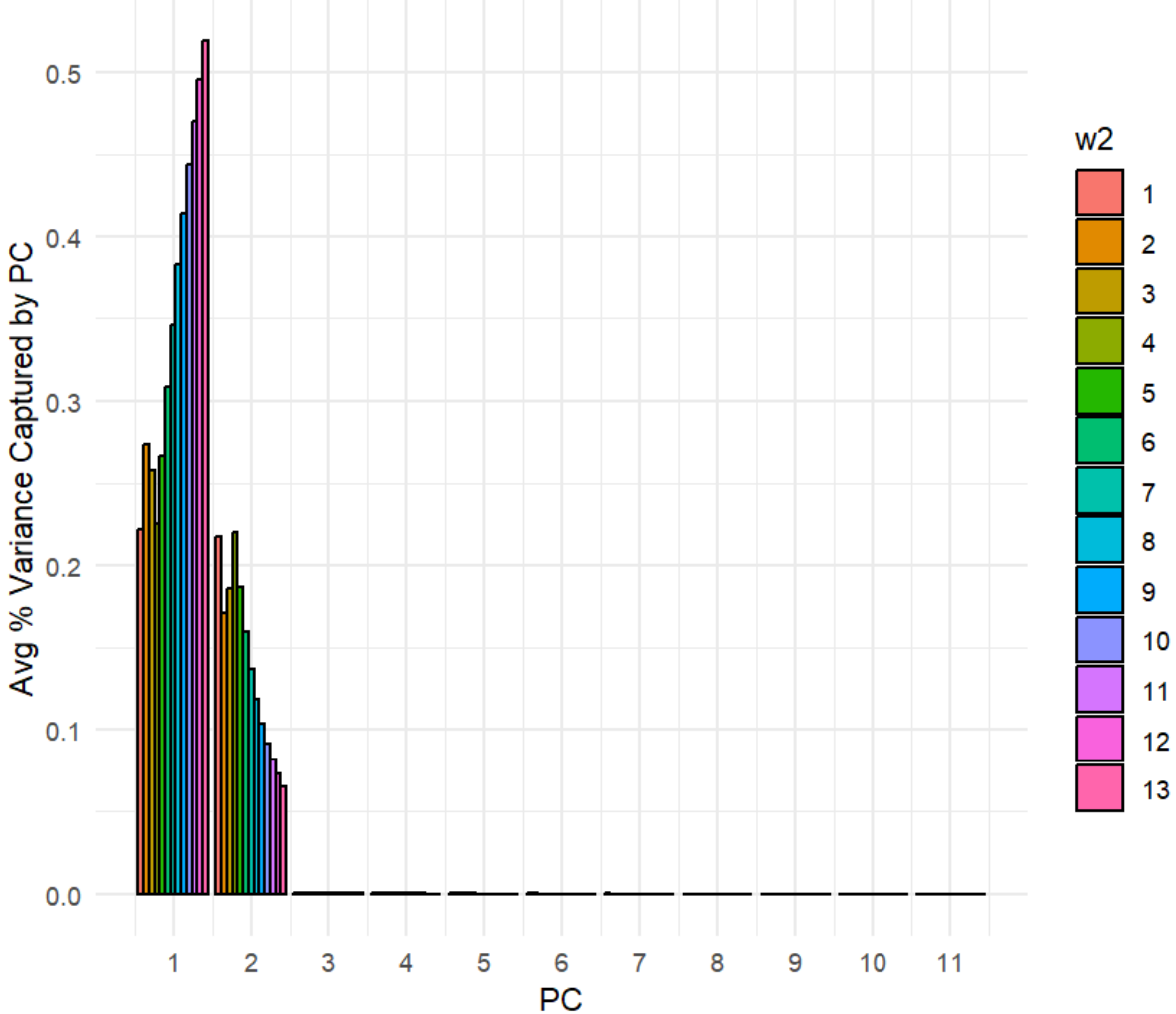


Figure 5: Example of scree plots depicting the average variance captured by all principal components in the conditional SWE of a 1-periodic series given several more-periodic series (as shown by the  $w_2$  values) over 100 samples.

## 4.2 Handling Noise

To handle noise when computing %DET, we fix the distance threshold to be greater than five times the standard deviation of Gaussian noise in each case of  $f_1$  and  $f_2$  [16]. To handle noise when computing  $\text{score}(f_1|f_2)$ , we perform two denoising methods on the discrete time series and on the resulting conditional SWE, respectively. To denoise the input series, we locally average every point in  $f_1$  and  $f_2$  by taking the mean of a window of points around it, and repeat this for each point. This process is called a simple moving average (SMA) and results in two averaged discrete signals. For our experiments, we pick  $P = 300$  points in  $f_1$  and  $f_2$ . Since  $f_1$  is  $w_1$ -periodic and we compute the conditional SWE on one cycle of  $f_1$ , we choose the SMA window size so that it at most one-third the number of points in one cycle of  $f_1$  ( $P/w_1$ ). In this way, we maintain a balance

of enough points for denoising while also maintaining the periodic structure of the time series.

To denoise the conditional SWE of  $f_1$  given  $f_2$ , we apply a similar process called mean shifting. That is, for each point  $\mathbf{v}_i \in \mathbb{R}^{M+1}$  in the point cloud, we average it with all of its neighbors  $\mathbf{v}_j$ , where  $\mathbf{v}_j$  is a neighbor of  $\mathbf{v}_i$  if the angle between these vectors is less than  $\pi/16$  [8, 20].

### 4.3 Shape and Noise Robustness of Our Score

We conduct similar experiments to those performed by Perea and Harer [19, §7.1] to analyze the stability of  $\text{score}(f_1|f_2)$  under small changes in Gaussian noise and periodic signal type of  $f_1$  and  $f_2$ . We consider periodic cosine, damped cosine, sawtooth, and square wave signals with varying levels of dampening (5%–80%) and Gaussian noise (0%–75%) applied to  $f_1$  and  $f_2$ . We plot one example of graphs for each of these cases (see Figure 6). For this experiment, we produce a  $4 \times 3$  grid plot, where each row corresponds to one signal type among cosine, damped cosine, square wave, and sawtooth signals from top to bottom, respectively. The first column is a plot of a 3-periodic series  $f_1$  and a 7-periodic series  $f_2$  with 5% Gaussian noise.

The second column in Figure 6 is a plot of  $\text{score}(f_1|f_2)$  against increasing embedding dimensions. This chart illustrates the application of Theorem 3.6. We vary  $M$  from 2 to 200, and include vertical lines at three embedding dimensions produced at three decreasing epsilon values. We define  $P = 300$  time series points, the simple-moving average (SMA) window to 10 points, the standard deviation of Gaussian noise to  $\sigma = 0.05$ , and  $M = \left\lceil \frac{2\pi}{w_2\epsilon} \right\rceil$  for  $\epsilon \in \{0.1, 0.05, 0.03\}$ . We maximize the number of embedding points  $N$  by fixing  $N = P$ .

The third column in Figure 6 shows the plots of average measures of  $\text{score}(f_1|f_2)$  against increasing values of  $w_2$  from  $w_1 = 3$  to 15. We average over 100 samples and plot the average measures along with their 95% confidence intervals (CIs). The  $p$ -values for all CIs corresponding to each value of  $w_2$  were less than 0.001. We obtain these using student's t-testing. We define the parameters for this plot the same as for that in column two, except we fix the SMA window to 19 points and increase the precision of our score by setting  $\epsilon = 0.0005$ .

### 4.4 Comparing Stability of Our Score and Percent Determinism

The goal of this experiment is to show experimentally that  $\text{score}(f_1|f_2)$  is more stable than %DET with respect to small changes in periodicity of  $f_2$  (i.e.,  $\frac{2\pi}{w_2}$ ), Gaussian noise (i.e., standard deviation  $\sigma$ ), and embedding dimension (i.e.,  $M$ ). The first set of results shows the average  $\text{score}(f_1|f_2)$  values against  $w_2$  for 5%, 10%, and 15% Gaussian noise. We report averages over 100 randomly generated samples and compute 95% CIs and  $p$ -values for each collection of  $w_2$  samples. All CIs produced  $p$ -values less than 0.001. These results are summarized in a  $2 \times 2$  grid, with the following plots (see Figure 7).

**Left:** average  $\text{score}(f_1|f_2)$  against  $w_2$  for all values of  $\epsilon$  (colored by value) for 5% noise ( $\sigma = 0.05$ ) over 100 samples.

**Middle:** Same as top left for 10% noise ( $\sigma = 0.10$ ).

**Right:** Same as top left for 15% noise ( $\sigma = 0.15$ ). We fix  $P = 300$ ,  $N = P$ , the SMA window size to 19 points,  $K = 2$ ,  $\epsilon = \{0.01, 0.03, 0.05\}$ ,  $w_1 = 2$ , and vary  $w_2$  from  $w_1$  to 15.

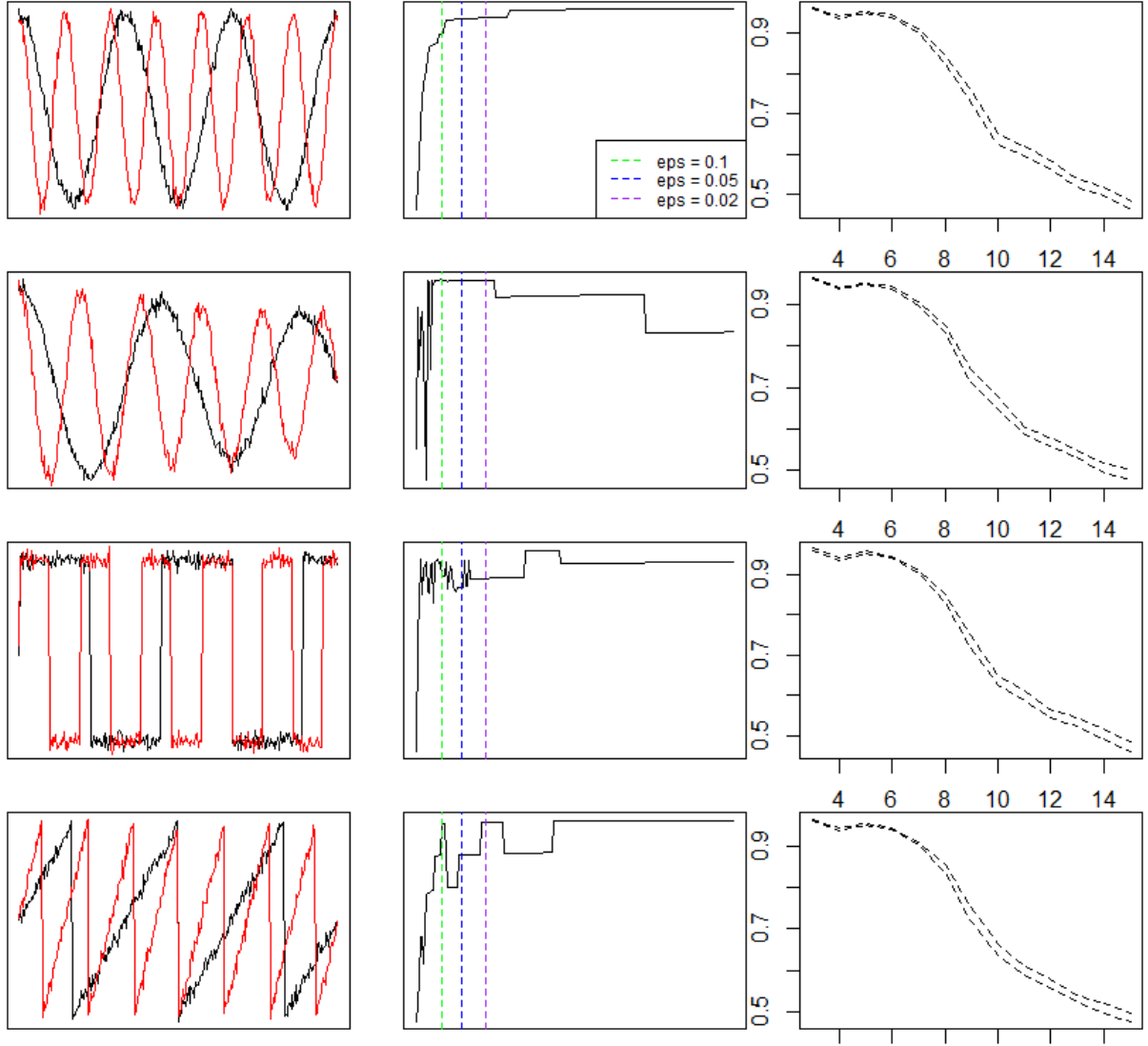


Figure 6: An example showing the robustness of  $\text{score}(f_1|f_2)$  to varying signal shapes and noise levels. We show 5% noisy time-series pairs (left column) of sinusoidal (top row), damped sinusoidal (second row), square wave (third row), and sawtooth (fourth row) structure. We illustrate an application of Theorem 3.6 in column two, where we plot  $\text{score}(f_1|f_2)$  for the pair of signals in the left column for increasing values of embedding dimension. We plot the minimum dimensions required to produce scores of  $\epsilon$  precision for decreasing values of epsilon as vertical lines in the plots (green, blue, and violet for  $\epsilon = 0.1, 0.05$ , and  $0.03$ , respectively). In column three, we plot the 95% confidence intervals produced from 100 randomly sampled scores for each periodicity of  $f_2$  as it diverges from that of  $f_1$ . We fix the minimum embedding dimension using  $\epsilon = 0.0005$ .

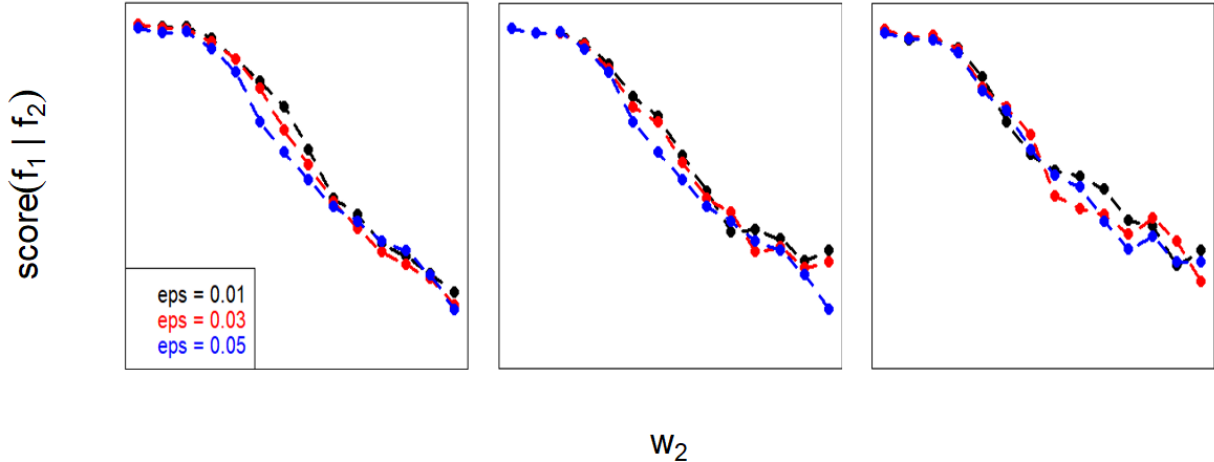


Figure 7: Robust sensitivity analysis of  $\text{score}(f_1|f_2)$  with respect to small changes in noise (5% left, 10% middle, 15% right), periodicity ( $w_2$  from  $w_1 = 3$  to 15), and input parameter  $\left(M = \left\lceil \frac{2\pi}{w_2\epsilon} \right\rceil\right)$ . Each plot shows the average score (y-axis values) over 100 generated samples against increasing periodicities of  $f_2$  (x-axis values).

The second set of results is for %DET vs  $w_2$  for 10% Gaussian noise. We define the input parameters for %DET as the time lag  $\tau$ , embedding dimension  $M$ , distance threshold  $\text{tol}$ , and the minimum number of points determining a diagonal line in the cross-recurrence matrix  $\mathcal{C}$ ,  $\text{minDL}$ . We again summarize our results in a  $2 \times 2$  grid, with the following plots (see Figure 8). For each case, we fix  $P = 300$ ,  $w_1 = 2$ ,  $\sigma = 0.10$  and increase  $w_2$  from  $w_1$  to 15.

**Top left:** average %DET against  $w_2$  for changing values of embedding dimension  $M$  (colored by value) and fixing all other parameters (described below) over 100 samples. We fix  $\tau = 3$ ,  $\text{minDL} = 2$ ,  $\text{tol} = 2\sigma + 2$ , and  $M = \{5, 6, 7\}$ .

**Top right:** Same as top left but for changing values of time lag  $\tau$  (colored by value). We fix  $M = 5$ ,  $\text{tol} = 2\sigma + 2$ ,  $\text{minDL} = 2$ , and  $\tau = \{3, 4, 5\}$ .

**Bottom left:** Same as top left but for varying the distance threshold  $\text{tol}$  (colored by value). We fix  $M = 5$ ,  $\tau = 3$ ,  $\text{minDL} = 2$ , and  $\text{tol} = 2\sigma + \{0.5, 1, 1.5, 2\}$ .

**Bottom right:** Same as top left but for varying the minimum diagonal line length  $\text{minDL}$  (colored by value). We fix  $M = 5$ ,  $\text{tol} = 3$ ,  $\text{tol} = 2\sigma + 2$ , and  $\text{minDL} = \{2, 5, 8\}$ .

Overall, %DET appears to be more stable with respect to small changes in distance threshold. However, %DET is much more sensitive to small changes in time lag, embedding dimension, and the minimum number of points defining a diagonal line in the cross-recurrence matrix. As well, our scoring function is much more stable with respect to small changes in noise and embedding dimension. Increasing the precision (i.e., decreasing  $\epsilon$ ) decreases  $\text{score}(f_1|f_2)$  for increasing periodicities of  $f_2$ . For sufficiently large enough periodicity of  $f_2$  and as noisiness of  $f_1$  increases, the scores start to overlap or cross. This is expected, as increased noise in  $f_1$  and oscillations in  $f_2$  compared to  $f_1$  changes the shape of the conditional SWE. Overall, our score decreases as the periodicity

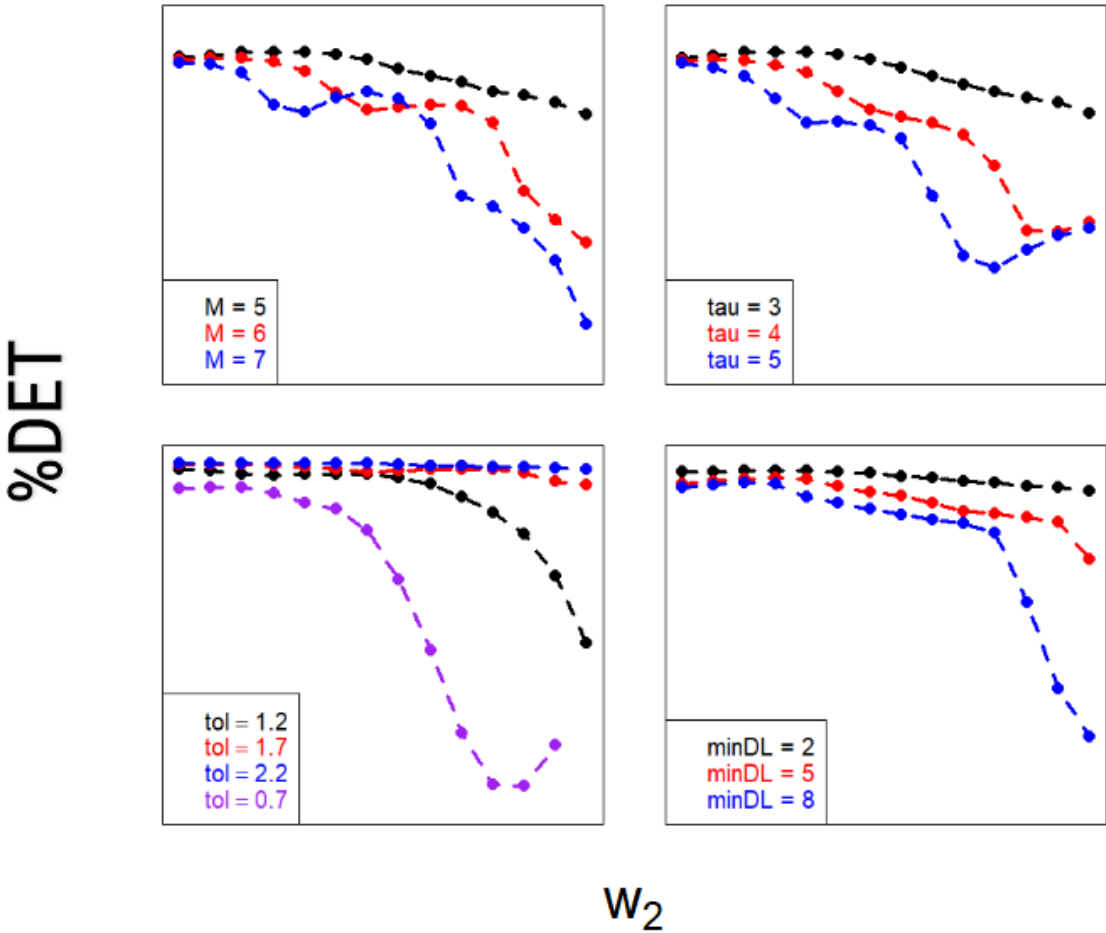


Figure 8: Robust sensitivity analysis of %DET for 10% noisy time series with respect to small changes in periodicity (increase  $w_2$  from  $3 = w_1$  to 15) and input parameters ( $\tau$ ,  $M$ ,  $\text{tol}$ , and  $\text{minDL}$ ). Each plot shows the average percent determinism (y-axis labels) over 100 generated samples against increasing periodicities of  $f_2$  (x-axis labels).

of  $f_2$  diverges from that of  $f_1$ . These results ultimately reveal the uniqueness of  $\text{score}(f_1|f_2)$  in its ability to measure periodicity similarity in a more stable manner that only requires one input parameter instead of four as is the case for %DET.

## 5 Discussion

Our conditional periodicity score is a similarity measure that is unique in its guaranteed theoretical stability under small changes in periodicity. Complementing our theoretical stability results, our score can be applied efficiently in practice with increased computational efficiency using PCA for dimension reduction. As well, our score is experimentally shown to be more robust than percent determinism when determining periodicity similarity, and only requires one input parameter compared to the four required by %DET. This parameter reduction is a highly favorable character-

istic of  $\text{score}(f_1|f_2)$  compared to %DET, as it reduces the number of biased decisions made during computation that can affect quantifications as shown in our experimental results. Our computations highlight the superior robustness of the conditional periodicity score in measuring periodicity similarity with respect to small changes in periodicity, noise, and embedding dimension.

While our measure provides a parameter-reduced quantification of periodicity similarity that maintains unique theoretical stability and increased robustness compared to %DET, we plan to obtain results comparing our measure to %DET on real data, as well as results when comparing synthetic time series of different types; e.g., cosine vs square-wave or sawtooth vs damped. We also plan to study how our score behaves when time series are relaxed to be generally periodic rather than  $L$ -periodic. In addition, we would like to obtain a stronger lower bound on the minimum number of embedding points required as a function of the optimal embedding dimension proven in Theorem 3.6. Finally, we would also like to obtain a lower bound on the minimum number of principal components needed so that the conditional periodicity score does not change much as discussed in Corollary 3.5. This result will help us to theoretically extend our work to other types of times series pairs whose expected conditional SWEs might not contain just two principal components capturing a majority of their variance.

## References

- [1] Henry Adams, Florian Frick, Sushovan Majhi, and Nicholas McBride. Hausdorff vs Gromov-Hausdorff distances, 2024. [arXiv:2309.16648](https://arxiv.org/abs/2309.16648).
- [2] Charu C. Aggarwal, Alexander Hinneburg, and Daniel A. Keim. On the surprising behavior of distance metrics in high dimensional space. In Jan Van den Bussche and Victor Vianu, editors, *Database Theory — ICDT 2001*, pages 420–434, Berlin, Heidelberg, 2001. Springer Berlin Heidelberg.
- [3] Luc Anselin. Dimension Reduction Methods (2): Distance Preserving Methods, 2020. Available as part of GeoDa: An Introduction to Spatial Data Science. URL: [https://geodacenter.github.io/workbook/7ab\\_mds/1ab7ab.html](https://geodacenter.github.io/workbook/7ab_mds/1ab7ab.html).
- [4] Eugene Oran Brigham and Richard E. Morrow. The fast Fourier transform. *IEEE Spectrum*, 4(12):63–70, 1967. [doi:10.1109/MSPEC.1967.5217220](https://doi.org/10.1109/MSPEC.1967.5217220).
- [5] Dmitri Burago, Yuri Burago, and Sergei Ivanov. *A Course in Metric Geometry*, volume 33 of *Graduate Studies in Mathematics*. American Mathematical Society, 2001.
- [6] Frédéric Chazal, Vin de Silva, Marc Glisse, and Steve Oudot. *The Structure and Stability of Persistence Modules*. SpringerBriefs in Mathematics. Springer Cham, 1 edition, 2016.
- [7] Frédéric Chazal, Vin de Silva, and Steve Oudot. Persistence stability for geometric complexes. *Geometriae Dedicata*, 173:193–214, 2014. [doi:10.1007/s10711-013-9937-z](https://doi.org/10.1007/s10711-013-9937-z).
- [8] Dorin Comaniciu and Peter Meer. Mean shift: a robust approach toward feature space analysis. *IEEE Transactions on Pattern Analysis and Machine Intelligence*, 24(5):603–619, 2002. [doi:10.1109/34.1000236](https://doi.org/10.1109/34.1000236).

[9] Derek de Beurs, Erik J. Giltay, Chani Nuij, Rory O'Connor, Remco F.P. de Winter, Ad Kerkhof, Wouter van Ballegooijen, and Heleen Riper. Symptoms of a feather flock together? An exploratory secondary dynamic time warp analysis of 11 single case time series of suicidal ideation and related symptoms. *Behaviour Research and Therapy*, 178:104572, 2024. [doi:10.1016/j.brat.2024.104572](https://doi.org/10.1016/j.brat.2024.104572).

[10] Shirley Duong, Tehran J. Davis, Heather J. Bachman, Elizabeth Votruba-Drzal, and Melissa E. Libertus. Dynamic structures of parent-child number talk: An application of categorical cross-recurrence quantification analysis and companion to Duong et al. (2024). *The Quantitative Methods for Psychology*, 20:137–155, 2024. [doi:10.20982/tqmp.20.2.p137](https://doi.org/10.20982/tqmp.20.2.p137).

[11] S.A. Dyer and J.S. Dyer. Cubic-spline interpolation. 1. *IEEE Instrumentation & Measurement Magazine*, 4(1):44–46, 2001. [doi:10.1109/5289.911175](https://doi.org/10.1109/5289.911175).

[12] Ian T. Jolliffe. *Principal Component Analysis*, volume 89. Springer-Verlag, 2002.

[13] Andjelka B. Kovačević, Aleksandra Nina, Luka č Popović, and Milan Radovanović. Two-Dimensional Correlation Analysis of Periodicity in Noisy Series: Case of VLF Signal Amplitude Variations in the Time Vicinity of an Earthquake. *Mathematics*, 10(22), 2022. [doi:10.3390/math10224278](https://doi.org/10.3390/math10224278).

[14] Musashi Ayrton Koyama, Facundo Memoli, Vanessa Robins, and Katharine Turner. Faster computation of degree-1 persistent homology using the reduced Vietoris-Rips filtration, 2024. [arXiv:2307.16333](https://arxiv.org/abs/2307.16333).

[15] Jean-Philippe Lachaux, Antoine Lutz, David Rudrauf, Diego Cosmelli, Michel Le Van Quyen, Jacques Martinerie, and Francisco Varela. Estimating the time-course of coherence between single-trial brain signals: An introduction to wavelet coherence. *Neurophysiologie Clinique/Clinical Neurophysiology*, 32(3):157–174, 2002. [doi:10.1016/S0987-7053\(02\)00301-5](https://doi.org/10.1016/S0987-7053(02)00301-5).

[16] Norbert Marwan, M. Carmen Romano, Marco Thiel, and Jürgen Kurths. Recurrence plots for the analysis of complex systems. *Physics Reports*, 438(5):237–329, 2007. [doi:10.1016/j.physrep.2006.11.001](https://doi.org/10.1016/j.physrep.2006.11.001).

[17] Nathan H. May, Bala Krishnamoorthy, and Patrick Gambill. A Normalized Bottleneck Distance on Persistence Diagrams and Homology Preservation Under Dimension Reduction. *La Matematica*, pages 1–23, 2024. [doi:10.1007/s44007-024-00130-0](https://doi.org/10.1007/s44007-024-00130-0).

[18] R. Mesbah, M. A. Koenders, A. T. Spijker, M. de Leeuw, A. M. van Hemert, and E. J. Giltay. Dynamic time warp analysis of individual symptom trajectories in individuals with bipolar disorder. *Bipolar Disorders*, 26:44–57, 2024. [doi:10.1111/bdi.13340](https://doi.org/10.1111/bdi.13340).

[19] Jose Perea and John Harer. Sliding Windows and Persistence: An Application of Topological Methods to Signal Analysis. *Foundations of Computational Mathematics*, 15:799–838, 2015. [arXiv:1307.6188](https://arxiv.org/abs/1307.6188), [doi:10.1007/s10208-014-9206-z](https://doi.org/10.1007/s10208-014-9206-z).

[20] Jose A. Perea, Anastasia Deckard, Steve B. Haase, and John Harer. SW1PerS: Sliding windows and 1-persistence scoring; discovering periodicity in gene expression time series data. *BMC Bioinformatics*, 16(1):257, 2015. [doi:10.1186/s12859-015-0645-6](https://doi.org/10.1186/s12859-015-0645-6).

[21] Christopher D. Riehm, Scott Bonnette, Justin L. Rush, Jed A. Diekfuss, Moein Kooheshtani, Gregory D. Myer, Grant E. Norte, and David A. Sherman. Corticomuscular cross-recurrence analysis reveals between-limb differences in motor control among individuals with ACL reconstruction. *Experimental Brain Research*, 242:355–365, 2024. [doi:10.1007/s00221-023-06751-1](https://doi.org/10.1007/s00221-023-06751-1).

[22] Floris Takens. Detecting strange attractors in turbulence. In David Rand and Lai-Sang Young, editors, *Dynamical Systems and Turbulence, Warwick 1980*, pages 366–381, Berlin, Heidelberg, 1981. Springer Berlin Heidelberg.

[23] Christopher J. Tralie and Jose A. Perea. (Quasi)Periodicity Quantification in Video Data, Using Topology. *SIAM Journal on Imaging Sciences*, 11(2):1049–1077, 2018. [doi:10.1137/17M1150736](https://doi.org/10.1137/17M1150736).

[24] Sarah Tymochko, Elizabeth Munch, Jason Dunion, Kristen Corbosiero, and Ryan Torn. Using persistent homology to quantify a diurnal cycle in hurricanes. *Pattern Recognition Letters*, 133:137–143, 2020. [doi:10.1016/j.patrec.2020.02.022](https://doi.org/10.1016/j.patrec.2020.02.022).

[25] Zhaokun Wei, Yaning Gao, Xiaoju Zhang, Xiaojun Li, and Zhifeng Han. Adaptive marine traffic behaviour pattern recognition based on multidimensional dynamic time warping and DBSCAN algorithm. *Expert Systems with Applications*, 238:122229, 2024. [doi:10.1016/j.eswa.2023.122229](https://doi.org/10.1016/j.eswa.2023.122229).

[26] Hasan Yiğit. Time Complexity of PCA 1. General Time Complexity of PCA, 08 2024. Posted on ResearchGate. [doi:10.13140/RG.2.2.12847.34728](https://doi.org/10.13140/RG.2.2.12847.34728).

[27] Yang Zhan, David Halliday, Ping Jiang, Xuguang Liu, and Jianfeng Feng. Detecting time-dependent coherence between non-stationary electrophysiological signals: A combined statistical and time-frequency approach. *Journal of Neuroscience Methods*, 156(1):322–332, 2006. [doi:10.1016/j.jneumeth.2006.02.013](https://doi.org/10.1016/j.jneumeth.2006.02.013).

[28] Wei Zhang, Satar Bakhsh, Kishwar Ali, and Muhammad Anas. Fostering environmental sustainability: An analysis of green investment and digital financial inclusion in China using quantile-on-quantile regression and wavelet coherence approach. *Gondwana Research*, 128:69–85, 2024. [doi:10.1016/j.gr.2023.10.014](https://doi.org/10.1016/j.gr.2023.10.014).